

THE ROLE OF FLOC DENSITY MEASUREMENTS IN ANALYZING  
SLUDGE DEWATERING CHARACTERISTICS

by

Catherine E. Arundel

Thesis submitted to the Faculty of the  
Virginia Polytechnic Institute and State University  
in partial fulfillment of the requirements for the degree of

MASTER OF SCIENCE

in

ENVIRONMENTAL ENGINEERING

APPROVED:

---

Dr. William R. Knocke,  
Chairman

---

Dr. John T. Novak

---

Dr. G. D. Boardman

March, 1986.

Blacksburg, Virginia

THE ROLE OF FLOC DENSITY MEASUREMENTS  
IN ANALYZING SLUDGE DEWATERING CHARACTERISTICS

by

Catherine E. Arundel

(ABSTRACT)

Floc density measurements may play a significant role in analyzing sludge dewatering characteristics. A laboratory technique was developed to measure this property by means of isopycnic centrifugation. Four laboratory sludges were subjected to a series of dewatering tests: gravity thickening, centrifugation, vacuum filtration, and high-pressure dewatering. Each sludge was analyzed for changing macro- and micro-properties during increasing stages of dewatering. It was concluded that sludge thickening rates are influenced by aggregate volume fractions, sludge density, suspension porosity, and the total surface area occupied by sludge aggregates. The extent of mechanical dewatering is impacted by similar parameters; namely, floc volume fractions, sludge density, cake porosity, and the total surface area occupied by sludge floc.

By interpreting the laboratory data, a model was formulated to describe changes in water distribution during the dewatering of sludges. This model includes a speculative view of the qualification and quantification of water-types.

## ACKNOWLEDGEMENTS

The author wishes to acknowledge Dr. G. D. Boardman and Dr. J. T. Novak for their respective contributions. Special thanks is extended to Dr. W. R. Knocke, whose guidance and interest were invaluable in completing this research. Also, \_\_\_\_\_ deserves grateful recognition for her moral and mental support.

Finally, the author wishes to thank \_\_\_\_\_ for his undying patience and much-needed encouragement.

## TABLE OF CONTENTS

	<u>Page</u>
ACKNOWLEDGEMENTS	iii
LIST OF FIGURES	vi
LIST OF TABLES	viii
 <u>Chapter</u>	
I. INTRODUCTION . . . . .	1
II. THEORETICAL CONSIDERATIONS . . . . .	3
Theory of Density Gradient Centrifugation . . . . .	3
Density Gradient Medium . . . . .	4
Centrifugation Considerations . . . . .	5
Sludge Behavior Principles . . . . .	5
Fundamental Definitions and Parameters . . . . .	6
Sludge Thickening Theory . . . . .	8
Settling Rates . . . . .	8
The Settling Process . . . . .	10
Vacuum Dewatering Theory . . . . .	13
Water Distribution Theory . . . . .	14
III. METHODS AND MATERIALS . . . . .	17
Materials . . . . .	17
Identification of Sludge Sources . . . . .	17
Percoll . . . . .	18
Methods . . . . .	20
Bulk Density . . . . .	20
Sludge Dry Solids Concentration . . . . .	20
Batch Settling Tests . . . . .	21
Ultimate Solids Concentration . . . . .	21
Vacuum Dewatering . . . . .	22
Centrifugation . . . . .	25
Pressure-Plate Test . . . . .	27
Methods Development . . . . .	29
Gradient Formation . . . . .	29
Sedimentation Process . . . . .	34
Floc Density Measurement . . . . .	35
IV. RESULTS AND DISCUSSION . . . . .	37
Gravity Thickening . . . . .	40
Bulk Density . . . . .	40
Settling Velocities and Aggregate Volume Index . . . . .	42
Mechanical Dewatering . . . . .	56
Important Sludge Relationships . . . . .	56
Parameters Affecting the Extent of Dewatering . . . . .	65
Particulate Structure Changes During	

	Dewatering . . . . .	67
	A Model of Water Distribution . . . . .	69
V.	CONCLUSION . . . . .	79
VI.	BIBLIOGRAPHY . . . . .	81
	APPENDIX A . . . . .	83
	APPENDIX B . . . . .	84

## LIST OF FIGURES

<u>Figure</u>		<u>Page</u>
1.	Diagram of Buchner funnel apparatus used for vacuum dewatering tests . . . .	23
2.	Determination of slope factor, "b", used for calculating specific resistance. Sample data taken from vacuum filter tests using unconditioned alum . . . .	26
3.	Diagram of pressure-plate device used for high-pressure mechanical dewatering of sludge samples . . . . .	28
4.	Calibration curve relating the density of Percoll solutions of varying density to measured refractive index . . . . .	32
5.	Determination of zone settling velocities at various concentrations of unconditioned alum sludge . . . . .	43
6.	Relationship between zone settling velocity and volume fraction of dry solids for conditioned alum sludge . . . .	44
7.	Relationship of zone settling velocity and dry mass solids concentration for six sludges . . . . .	47
8.	Relationship of zone settling velocity and sludge aggregate volume fraction for the six sludges examined in this study . . . . .	50
9.	Observed experimental data relating thickening constant (k) to the aggregate volume index . . . . .	53
10.	Effect of applied pressure on the extent of sludge dewatering observed . .	59
11.	Relationship between measured bulk density and dry solids concentration during the dewatering of ferric hydroxide sludge . . . . .	61
12.	Relationship between measured bulk density and dry solids concentration during the dewatering of unconditioned and conditioned alum sludges . . . . .	62

13.	Relationship between measured bulk density and dry solids concentration during the dewatering of lime sludge . .	63
14.	Effect of centrifugal acceleration on extent of sludge dewatering observed . . . . .	72

## LIST OF TABLES

<u>Table</u>	<u>Page</u>
1.	Physical Properties of Percoll . . . . . 19
2.	Methods of Determination for Various Fundamental Sludge Properties . . . . . 38
3.	Calculated Values of Various Fundamental Sludge Micro-Properties . . . . . 39
4.	Properties of Sludges After Gravity Thickening . . . . . 41
5.	Equations Relating Interface Settling Velocities to Aggregate Volume Index from Figure 7 . . . . . 51
6.	Equations Relating Interface Settling Velocities to Aggregate Volume Index from Figure 8 . . . . . 54
7.	Summary of Relationships Between Impor- tant Sludge Micro-Properties and Corresponding Sludge Thickening Characteristics . . . . . 57
8.	Calculation of $\phi_f$ for Corresponding %SS at Two Stages of Mechanical Dewatering . 68
9.	Calculated Values of Volume Fractions Applicable to Quantification of Sludge Water-Types . . . . . 76



## I. INTRODUCTION

Sludge dewatering and disposal issues greatly impact water and wastewater treatment facilities due to the problem of economically producing a minimum volume, highly dewatered sludge residue. This problem has become urgent by an ever-increasing production of sludge, plus limited ultimate disposal sites and/or options. This urgency must be met by efforts to better understand the fundamental principles governing sludge dewatering processes. With an increased knowledge of the fundamentals, dewatering techniques can be optimized.

Past dewatering research studies have emphasized the macro-properties of sludge. For example, measurements of bulk density and dry solids concentration have been used to analyze and compare sludges. Many times, this has resulted in the development of conclusions related to dewatering characteristics that were specific to a single sludge or subset of sludges. Without a reliable technique for measuring sludge micro-properties, scientists have been limited in their ability to fully explain observed dewatering phenomena.

The next step in furthering present knowledge, then, is the development of accurate procedures for measuring micro-properties. With this additional information, a

more thorough examination of sludge behavior during gravity and mechanical dewatering should be possible.

Given the above discussion, the objectives of this study were:

1. to develop a method for the measurement of an important micro-property, sludge floc density;
2. to correlate changes in micro- and macro-properties with different sludge dewatering characteristics; and
3. to formulate a descriptive model for the distribution of water during dewatering.

## II. THEORETICAL CONSIDERATIONS

In order to further develop the specific objectives of this research, certain theoretical considerations must be considered. Therefore this chapter combines a formal literature review with the discussion of theory and terms that are important for the analysis of results. The two topics covered are Theory of Density Gradient Centrifugation and Sludge Behavior Principles.

### Theory of Density Gradient Centrifugation

Density gradient centrifugation has been traditionally used by biochemists for the separation of cells, viruses, and subcellular particles. Particle separation is accomplished by two methods. The first method is called rate-zonal centrifugation, where separation is based on size differences between particles. According to Stokes' Law (1), larger particles move faster through a gradient than smaller particles. A measurement of sedimentation rate serves to differentiate between particles.

The second method of particle separation by centrifugal means is isopycnic centrifugation. In this procedure, particles settle to an equilibrium position, called the isopycnic point. The density of the particle is

equal to the density of the gradient medium at this isopycnic point. This method of separation is a function only of particle density, and is independent either of particle size or rate of sedimentation (2). For this reason, isopycnic centrifugation was considered applicable to floc density determination. However, attempts to adapt this technique to sludges have been limited by the incorrect choice of media and improper centrifugation procedures (3). In developing a valid technique, media and centrifuge considerations must be addressed.

#### Density Gradient Medium

An ideal gradient medium must possess certain characteristics (2). Those most important in measuring sludge floc densities are presented below. The medium should:

- cover a wide range of densities,
- be iso-osmotic throughout the gradient, and exert a low osmotic pressure,
- be non-toxic,
- have a low viscosity, and
- be able to form self-generated gradients by centrifugation at low g-forces.

Past researchers attempted to use salt and sucrose solutions for density gradient formation. These media were limited in their ability to provide low-pressure,

iso-osmotic gradients. Furthermore, sucrose was unable to form self-generated, continuous gradients (4,5).

Potential problems associated with saline and sucrose necessitated the search for a new density gradient medium. Recently, a substance known as Percoll has been introduced for density determinations, and experimental results have confirmed its applicability (3). This material covers a wide range of densities, meets osmotic pressure requirements, and is flexible in its method of gradient formation. A more thorough description of Percoll and its properties are presented in Methods and Materials.

#### Centrifugation Considerations

Regardless of the medium used, if proper centrifugation is not applied, accurate floc density measurements are not possible. Three important considerations are the type of centrifuge (swinging-bucket versus angle-head), the time and the force of centrifugation. These subjects are addressed in Methods Development.

#### Sludge Behavior Principles

The examination of sludge behavior requires an understanding of certain basic principles. For the purpose of clarification, then, this section presents

relevant sludge properties and definitions.

Furthermore, brief discussions of theories concerning sludge thickening, mechanical dewatering, and water distribution are included.

### Fundamental Definitions and Parameters

The two raw materials that combine to form sludge are water and dry matter. These substances are present in three species: primary particles, floc, and aggregates. Primary particles are composed of dry sludge and tightly bound water. Floc are formed when these particles cluster together, enclosing water within their structure. The floc may join together, entrapping more water. This floc network constitutes an aggregate (6).

Certain parameters are essential to fundamental sludge studies. Bulk density ( $\rho_b$ ) measures the weight per unit volume of a sludge slurry. The slurry may consist of any combination of particles, floc, aggregates and/or supernatant. Each of the three defined species possesses its own characteristic density. Although bulk densities may be measured experimentally in the laboratory, individual species measurements are more complicated. Dry particle density ( $\rho_k$ ) may be calculated using the following equation (3):

$$\frac{100}{\rho_b} = \frac{(100 - C)}{\rho_w} + \frac{C}{\rho_k} \quad (1)$$

where  $C$  = mass solids concentration, (% by weight)  
 $(100 - C)$  = sludge water content, (% by weight)  
 $\rho_w$  = density of water, (1.0 g/ml)

With the centrifugal laboratory technique developed in this research, floc density ( $\rho_f$ ) may now also be measured. Aggregate density ( $\rho_a$ ), however, must be calculated from the following equation (3):

$$\rho_a - \rho_w = \frac{(\rho_k - \rho_w)}{AVI} \quad (2)$$

where the parameter AVI constitutes the aggregate volume index. A discussion of AVI, its method of determination, and its significance in sludge thickening and dewatering are presented in the section of this chapter covering Sludge Thickening Theory.

A second relevant sludge parameter is the volume fraction of a species. For instance, the volume fraction of dry solids ( $\phi_k$ ) defines the volumetric portion of a sludge occupied by dry solids. The volume fraction of dry solids is calculated by the expression (3)

$$\phi_k = \frac{C}{\rho_k} \quad (3)$$

Similarly, floc volume fraction ( $\phi_f$ ) is computed from

$$\phi_f = \frac{C}{\rho_f} \quad (4)$$

The volume fraction of aggregates ( $\phi_a$ ) may be determined by the following:

$$\phi_a = (AVI)\phi_k \quad (5)$$

### Sludge Thickening Theory

The object of efficient thickening is to obtain a high dry solids content in a short time period. Thus, quantification expressions for the extent and rate of gravity thickening are important. The extent of thickening is a function of the amount of water removed during settling and is expressed as the solids concentration of thickened sludge. The rate of settling is a more complicated topic that merits further discussion.

Settling Rates. Particle dynamics are an important consideration when calculating settling rates. The interaction of complicated hydrodynamic forces between a particle and a fluid determine the velocity at which the



particle will travel.

Fundamental settling rate theory began with Stokes' Law (7):

$$V_o = \frac{D^2 g (\rho_p - \rho_w)}{18 \mu} \quad (6)$$

where  $g$  = gravitational force, (m/s<sup>2</sup>)

$\rho_p$  = particle density, (g-s<sup>2</sup>/m<sup>4</sup>)

$\rho_w$  = density of fluid, (g-s<sup>2</sup>/m<sup>4</sup>)

$D$  = particle diameter, (m)

$\mu$  = solution viscosity, (g-s/m<sup>2</sup>)

This law expresses the terminal velocity of a single spherical particle in an infinite fluid under laminar flow conditions. However, ideal conditions do not apply during sludge settling. For example, interferences from surrounding particles, turbulence, viscous flow and wall effects, invalidate certain assumptions made in Stokes' Law. Many modifications of Equation 6 have been made by various authors in an attempt to include these forces. The work of Richardson and Zaki (8) culminated in an expression for sludge settling velocity ( $V_s$ ) that proved valid with experimental data. Their formula was as follows:

$$V_s = V_o e^{4.65} \quad (7)$$

where  $V_S$  = sludge settling velocity, (m/hr)

$V_O$  = Stokes' settling velocity, (m/hr)

$e$  = sludge porosity, dimensionless

Equation 7 was the basis for further modification by Michaels and Bolger (6) and Javaheri and Dick (7). Their modified expression dealt with sludge as a slurry of aggregates with flow moving around and through the aggregates. According to both sets of researchers, sludge settling velocity may be calculated as:

$$V_S = V_O (1 - \phi_a)^{4.65} \quad (8)$$

Equation 8 incorporates flow conditions, thereby emphasizing the role of the fluid, as well as the floc fraction.

The Settling Process. The fate of sludge aggregates during settling is now considered. As an aggregate descends, the surrounding fluid creates pressure differences between its top and bottom that forces the particle downward. As the fluid displaces, it meets forces of resistance that must be overcome for settling to continue. Resistance is a function of two types of drag forces: form and surface. Form drag force depends on particle shape and is due to the

pressure differential between its top and bottom. Surface drag force is the result of friction along the particle's surface.

Certain sludge parameters aid in characterizing the sludge. The Stokes' Law settling velocity ( $V_o$ ) has been considered an indication of sludge particle size. The aggregate volume index (AVI) measures the water content associated with sludge aggregates. This term was developed by Javaheri and Dick (7) with ideas incorporated from Michaels and Bolger (6). The AVI evolved from the following relation:

$$\frac{\rho_a - \rho_w}{\phi_a} = \frac{\phi_k}{\phi_a} (\rho_k - \rho_w) = \frac{1}{AVI} (\rho_k - \rho_w) \quad (9)$$

Mathematically, the AVI represents the volume fraction of aggregates divided by the volume fraction of dry solids. The AVI of a sludge may either remain constant or change during settling. A constant AVI indicates aggregates retain their characteristic water content during settling. A decreasing AVI indicates a release of water from the aggregate during thickening (7). A useful expression for calculating AVI and  $V_o$  is (3):

$$V_s^{1/4.65} = V_o^{1/4.65} - V_o^{1/4.65} (AVI) \phi_k \quad (10)$$

A plot of  $v_s^{1/4.65}$  versus  $\phi_k$  yields a straight-line relationship, from which both the AVI and  $V_o$  may be calculated. A characteristic plot and a sample calculation are included in the Results and Discussion section.

The fate of sludge particles is also described by examining differential zones of settling. Physically, these zones represent the surface, intermediate, and bottom regions of a settling basin or column. The upper region is characterized by hindered settling, where all particles in the suspension travel at one settling velocity, unaffected by previously settled sludge. In the middle region, particles begin to decelerate due to an increase in solids concentration from the sludge blanket. Finally, a zone of compression forms where particles deposit and are compacted from the weight of overlying particles and supernatant (9).

At present, certain gaps exist in settling theory. The species of sludge present during thickening is an important consideration. However, no concrete evidence has yet been offered to define whether the floc or the aggregate is the dominant species present during thickening. The greatest gap in knowledge is in the determination of factors that influence settling characteristics. Past studies emphasized the mass concentration of solids as a key to explaining changes

in settling velocity. This concept is challenged by researchers who promote sludge volume as a major influence on settling characteristics (10). As this research will show, the latter relation is a relevant one that leads to the identification of other important relationships in sludge thickening.

#### Vacuum Dewatering Theory

Similar to gravity thickening, the object of mechanical dewatering is to achieve a sludge of high solids concentration in a short period of time. Therefore, both the rate and extent of dewatering are also important in mechanical dewatering systems.

Past literature concentrated on rate studies to improve dewatering performance (11). A useful parameter for such studies is the specific resistance ( $r^*$ ) which measures the resistance to fluid flow exerted by a cake of unit weight dry solids per unit area. In simpler terms,  $r^*$  indicates how easily a sludge is dewatered when a pressure differential is applied to the sludge cake. The formula for calculating  $r^*$  is based on Darcy's equation for fluid flow through a porous media. The formula and method of calculation are presented in Materials and Methods. A detailed derivation has also been presented by Vesilind (12).

A comparison of sludge parameters in the literature led to the conclusion that sludge floc size had the

greatest effect on the rate of sludge dewatering (11). When mean floc size increased,  $r^*$  values decreased, indicating an improvement in the rate of sludge dewatering. This idea was recently challenged by studies that promote other floc properties as key factors (13). Specifically, size distribution and density were introduced as important parameters in determining both rate and extent of mechanical dewatering. Thus, mechanical dewatering theory was extended to consider the extent as well as the rate of dewatering. In addition, consideration of different sludge micro-parameters was initiated.

Future studies require the investigation of a wider variety of sludge properties as measurement techniques develop. Also, attention should focus on the extent of mechanical dewatering to gain insight into the process.

#### Water Distribution Theory

Two theories describing water distribution within a sludge are presented to establish fundamental principles needed for discussion.

The first theory was developed by Vesilind (12), who defined the following four categories of water in a sludge slurry:

1. Free water - unbound water, not held to sludge particles; removed by gravity thickening.

2. Floc water - water held within the floc and removed by mechanical dewatering.

3. Capillary water - water bound to sludge particles by surface tension and attractive forces; removed by floc deformation and compression.

4. Bound water - water held to floc particles by chemical forces; not removed by mechanical dewatering.

Vesilind suggested these categories could be quantified by high-speed centrifugation. He hypothesized that a plot of dry solids concentration versus centrifugal acceleration speed would reveal points of deflection, signifying the transition between these water-types.

A second theory was published by Möller (14), who considered dewatering characteristics to be a function of sludge geometry, sludge properties, and, more importantly, the intensity of the binding forces of water. Möller stressed the importance of energy requirements for breaking these binding forces. The following categories of water were defined:

1. Interspace water - a type of external water having the weakest attachment to sludge particles; composes the majority of water in an unthickened sludge.

2. Adhesion and capillary waters - external waters with intermediate binding forces; together, they account for the second largest category of water.

3. Adsorption water - most strongly bound of the

external water-types; forms a protective layer around the particles and constitutes only a small fraction of the total water present; can only be removed by thermal forces.

4. Internal water - constitutes floc or particle moisture and chemically bound water; removed by transforming internal water to external water using biological or thermal means.

Both theories consider binding forces and methods of removal important in qualifying water types. A useful model of water distribution should also discuss a means of quantification. This research addresses both qualification and quantification when developing a model of water distribution within a sludge.



### III. MATERIALS AND METHODS

This chapter outlines the experimental materials and methods used for data collection. In addition, a Methods Development section is included for the description of floc density measurement techniques.

#### Materials

##### Identification of Sludge Sources

Four sludges were used for laboratory testing. The sludges are characterized below.

1. The ferric hydroxide sludge was produced in the laboratory by adding 3 grams per liter (g/L) of  $\text{FeCl}_3$  to tap water and subsequently precipitating  $\text{Fe}(\text{OH})_3(\text{s})$  at pH 8.0 by sodium hydroxide addition. The tap water originated in the New River.

2. Unconditioned alum sludge was obtained from a thickening basin at the Radford Arsenal Water Treatment Plant in Radford, Virginia. This water was also supplied by the New River.

3. The conditioned alum sludge was produced in the laboratory by adding 14 mg/L of Betz 1120 polymer to one Liter of alum sludge obtained from Radford Arsenal.

4. The lime sludge (essentially  $\text{CaCO}_3(\text{s})$ ) was obtained from a water softening treatment plant located in Columbia, Missouri.

### Percoll

Percoll (trade-name, marketed by Pharmacia Fine Chemicals AB of Sweden) is a modified colloidal silica with specific physical properties, listed in Table 1. This substance was originally used in the biological field for separating particles by density gradient centrifugation. The colloidal silica are coated with Polyvinylpyrrolidone (PVP) to provide colloidal stability and protect biological specimens from toxins (2). In this research, Percoll was used to generate density gradients for measuring the density of sludge floc.

A number of properties make Percoll suitable for measuring floc density. First, it may be diluted or concentrated to cover a density range of 1.0 - 1.3 grams per milliliter (g/mL). Second, Percoll possesses a low osmotic pressure and sustains iso-osmotic conditions which prevents the sludge floc from fracturing. Third, this medium is non-toxic and of low viscosity. Finally, the method of gradient formation is flexible. Step gradients may be manually-layered or the Percoll may be centrifuged for self-generated gradient formation (2). A thorough discussion of density determination and dilution/concentration techniques with Percoll is provided in the Methods Development section of this chapter.

TABLE 1  
Physical Properties of Percoll (2)

Property	Specifications
Composition	silica sol with PVP coating
Density	$1.130 \pm 0.005$ g/mL
Conductivity	1.0 mS/cm
Osmolality	20 mOs/kg H <sub>2</sub> O
Viscosity	$10 \pm 5$ cP at 20°C
pH	$8.9 \pm 0.3$ at 20°C
Refractive Index	$1.3540 \pm 0.005$ at 20°C

## Methods

### Bulk Density

The bulk density of each sludge sample was determined using a glass pycnometer. The pycnometer provided a precise measurement of density.

For sludge bulk density measurements, the pycnometer was first filled with distilled water at room temperature, then weighed to the nearest 0.001 gram (g). Weights were taken a minimum of three times, or until acceptable reproducibility was achieved. The pycnometer was then emptied, dried, and filled with sludge. The weighing procedure was repeated. When representative values were obtained, the bulk density was calculated using the following formula:

$$\rho_b = \frac{\text{net weight of sludge} \times \text{unit density of water}}{\text{net weight of water}} \quad (11)$$

where  $\rho_b$  = bulk density of sludge, (g/mL)

The unit weight of water for this study was taken to be essentially 1.0 g/mL at 20°C.

### Sludge Dry Solids Concentration

Dry solids concentration was reported on a percentage by weight basis. First, an aluminum pan was weighed. A sample of sludge was placed in the pan and the combined weight recorded. The pan and sludge sample were then placed in a 103°C oven overnight, or until a

constant weight was achieved. After cooling, the pan plus dried sludge were reweighed and the weight recorded. Equation 12 was used to calculate percent dry solids (% SS):

$$\% \text{ SS} = \frac{\text{net weight of dry sample} \times (100)}{\text{net weight of wet sample}} \quad (12)$$

### Batch Settling Tests

Batch settling tests were performed by tracking the movement of a sludge/water interface as it moved downward in a one Liter, 0.5 meter column. A series of dilutions was made for each sludge sampled. After uniform mixing, an interface appeared between the settling sludge and the dilution water. Using a stopwatch, the settling time with respect to column height was recorded.

### Ultimate Solids Concentration

The sludge and dilution water mixtures used in the batch settling tests were allowed to settle for 24 hours. This time limit was defined as an index of the maximum or ultimate dry solids concentration that might be obtained purely by gravity thickening. The height of the settled sludge in each column was noted and used to calculate the ultimate solids concentration of gravity thickened sludge ( $C_u$ ) according to the following mass balance equation:

$$C_u = \frac{C_o H_o}{H_u} \quad (13)$$

where  $C_u$  = final solids concentration of thickened sludge, (%)

$C_o$  = initial solids concentration, (%)

$H_o$  = initial height of sludge and dilution water, in centimeters (cm)

$H_u$  = final height of thickened sludge, (cm)

### Vacuum Dewatering

Vacuum dewatering was one of three procedures used in this study to mechanically dewater sludge samples. A Buchner funnel apparatus (shown in Figure 1) was used. Sample sludge volumes of 100 mL were poured into the funnel and allowed 30 seconds to stabilize. (With certain sludges, this stabilization period was not possible, because the sample began passing through the filter almost immediately.) A pressure of 15 millimeters (mm) of mercury was applied to the sample. Water passed through the #40 ashless filter paper and was collected in a graduated cylinder. The volume of filtrate and corresponding time of filtration were recorded. Vacuum dewatering was discontinued when the sludge cake failed, i.e., when large cracks appeared across the cake and the pressure differential across the cake began to drop.

Data from Buchner funnel tests were used in

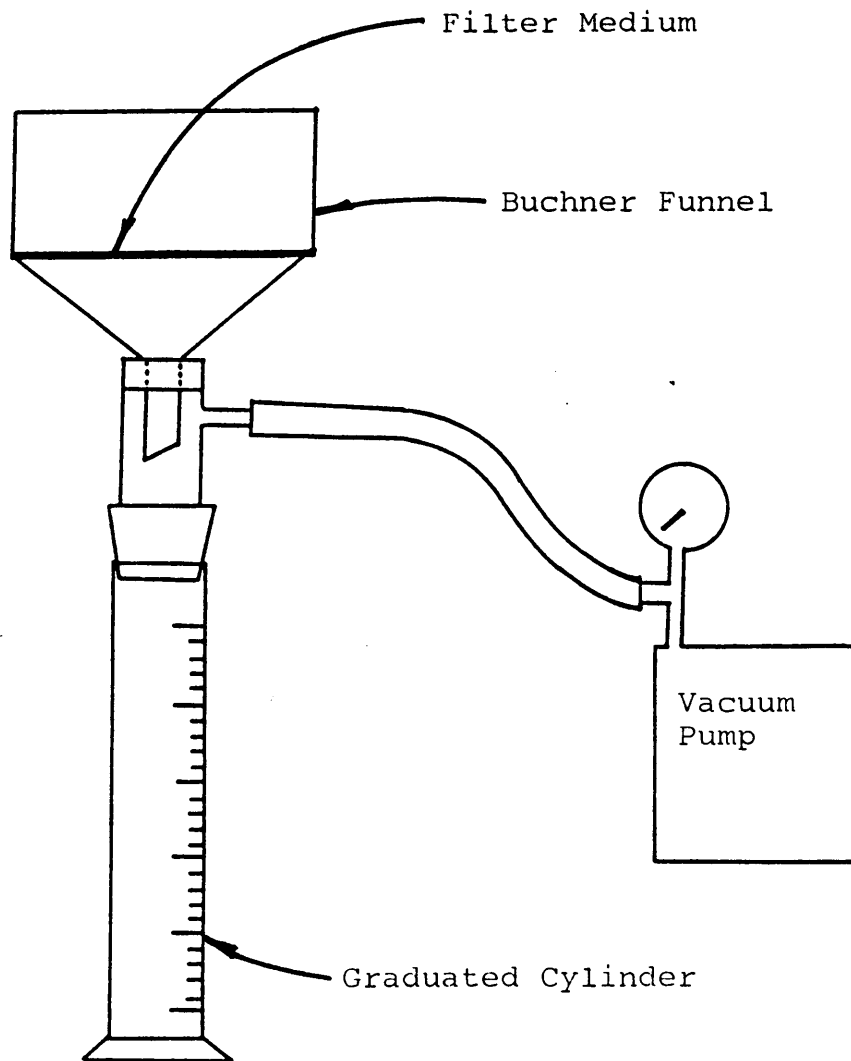


Figure 1: Diagram of Buchner Funnel Apparatus Used For Vacuum Dewatering Tests

Equation 14 to calculate the specific resistance of each sludge:

$$r^* = \frac{2A^2 b P_t}{c \mu} \quad (14)$$

where  $r^*$  = specific resistance, meters per kilogram  
(m/kg)

$A$  = surface area of filter paper, (m<sup>2</sup>)

$P_t$  = applied pressure differential across sludge  
cake, Newtons per square meter (N/m<sup>2</sup>);

$\mu$  = filtrate viscosity, Newton-seconds per  
square meter (N-s/m<sup>2</sup>)

$c$  = mass solids concentration parameter,  
kilograms per cubic meter (kg/m<sup>3</sup>)

$b$  = slope of a plot relating time and volume of  
vacuum dewatering, seconds (s)

The value for  $c$  depended upon the mass of solids deposited on the filter during dewatering and was calculated by:

$$c = \frac{C_o C_f}{100(C_f - C_o)} \quad (15)$$

where  $C_o$  = initial solids concentration, (%)

$C_f$  = final dewatered solids concentration, (%)



To calculate  $b$ , the data from Buchner funnel tests were used to plot time/volume ( $t/v$ ) versus volume ( $v$ ) for each sludge. Figure 2 shows a typical plot for the unconditioned alum sludge tested. The slope of the linear portion of the curve was used to calculate  $b$ .

At periodic intervals of dewatering, the process was stopped and representative dry solids concentrations and bulk densities were measured. In this way, changes in sludge properties due to dewatering were monitored.

#### Centrifugation

Dewatering by centrifugal means was the second method used to accomplish mechanical dewatering. During this process, the high-speed rotation of the centrifuge created forces that separated solids and liquid, i.e., sludge and supernatant. This separation occurred as a result of density differences between the two phases (15).

For each sample, two centrifuge tubes were filled with the slurry, then balanced by filling two additional tubes with enough tap water to reach an equivalent weight. The four tubes were inserted into a Beckman centrifuge with an angle-head rotor. The sludge samples were subjected to specified centrifuge speeds for 15 minutes each. For each speed, characteristic bulk density and solids concentration measurements were taken.

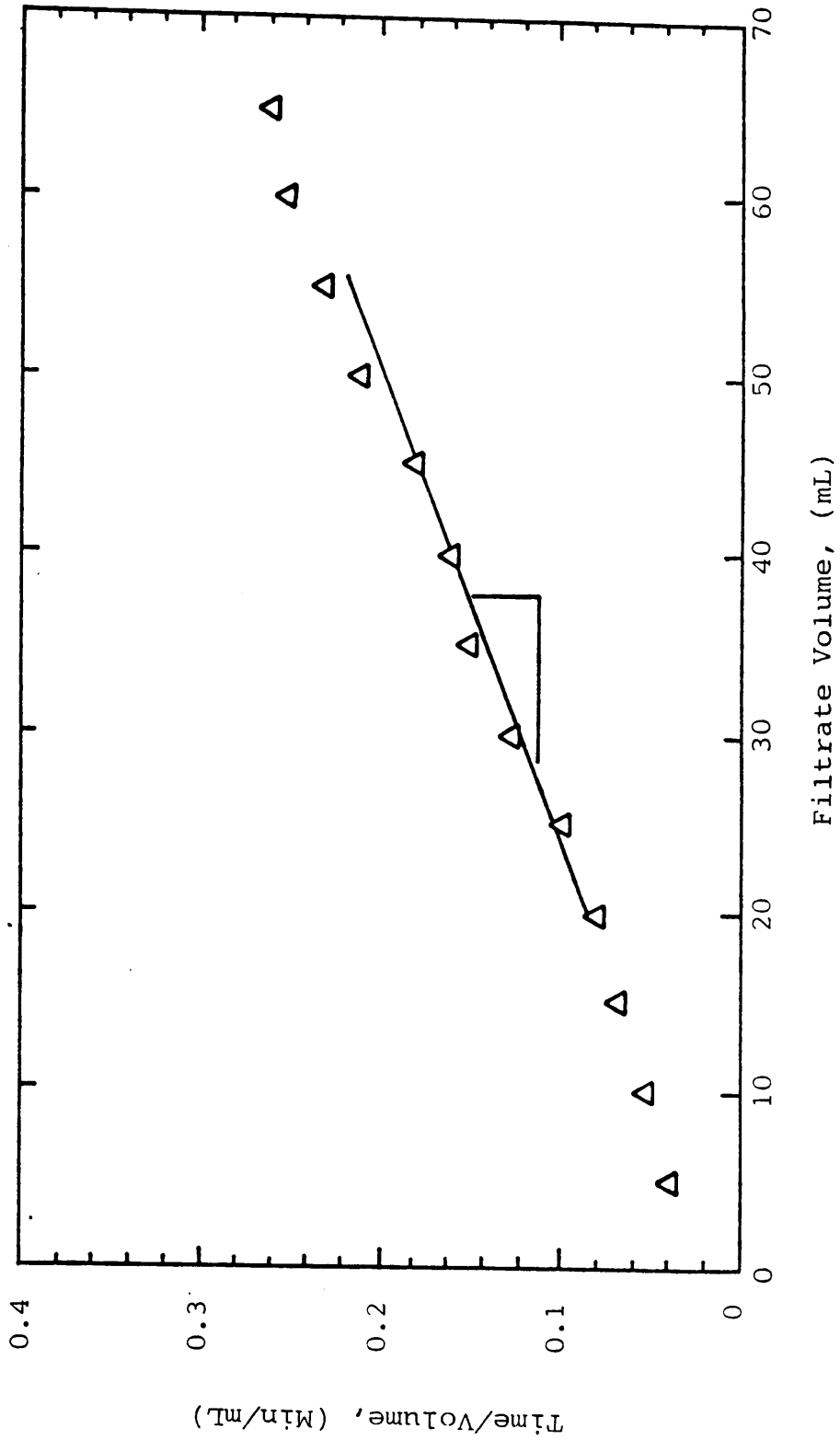


Figure 2: Determination of Slope Factor, "b", Used for Calculating Specific Resistance. Sample Data Taken From Vacuum Filter Tests Using Unconditioned Alum

### Pressure-Plate Test

The third dewatering method used was a high-pressure technique which used a pressure-plate device. This procedure, used by agronomists to remove water from soils, was able to dewater the sludge in an undisturbed state. The applied pressure was equally distributed throughout the sample, providing uniform dewatering throughout the floc matrix (16). A further advantage of this technique was its wide range of pressures. Sludges were subjected to pressures as high as 15 bars, well above that exerted by a vacuum filter or a high-speed centrifuge.

The high-pressure dewatering apparatus is depicted in Figure 3. The ceramic plates were soaked for 12 hours in a water bath. This saturation served to remove air from the pores of the plates. The sludge samples were then arranged on the plates inside aluminum rings measuring 25 cubic centimeters. One to three samples of each sludge were tested, depending on the available sample volume. The chamber was capped and the bolts tightened to ensure that no air leakage occurred. The chamber air pressure was adjusted to three specific differentials: 1 bar, 3 bars, and 15 bars of pressure. Sludge dewatering was complete when each sample reached a constant weight and no further water dripped from the

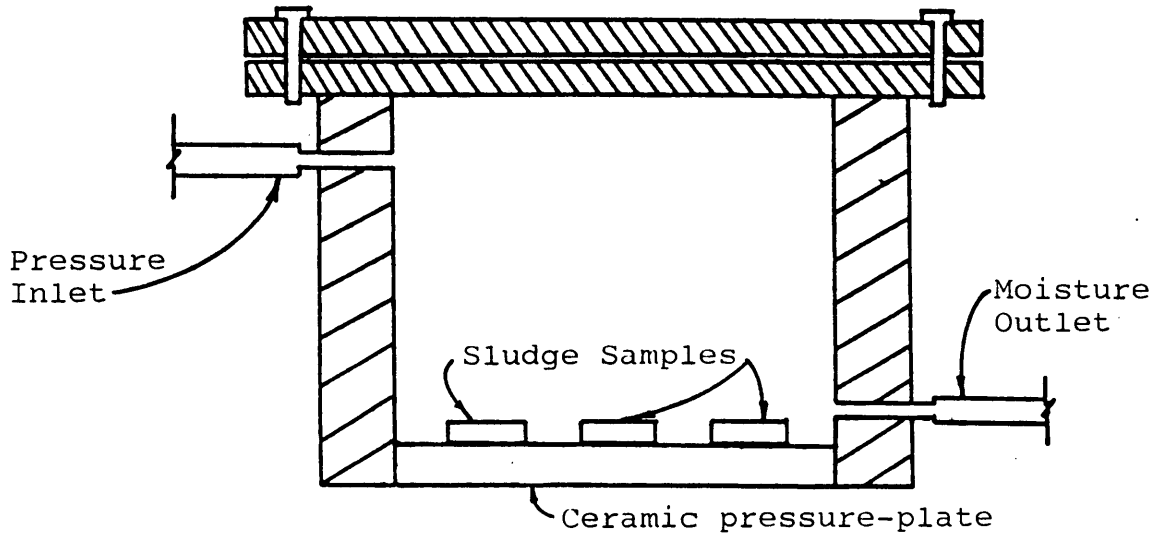


Figure 3: Diagram of Pressure-Plate Device Used for High-Pressure Mechanical Dewatering of Sludge Samples

outlet. Upon completion of the test, each sample was measured for bulk density and solids concentration. To obtain representative measurements, replicates were measured individually. These values were averaged to obtain a single bulk density and dry solids concentration for a particular sludge at a given pressure.

### Methods Development

One objective of this research is to develop a method for the measurement of sludge floc density. Three procedural units are outlined to explain this method of measurement.

#### Gradient Formation

First, a density range was estimated that included the minimum and maximum values predicted for a particular sludge. Density gradients differed by no less than 0.01 g/mL. For example, gradients of 1.06, 1.07, 1.08, 1.09, and 1.10 g/mL were used for characterizing ferric hydroxide sludge. Floc gradients were created by diluting or concentrating the stock solution of Percoll. From Table 1, the density of the stock solution was 1.13 g/mL.

Percoll and distilled water were mixed to obtain a solution of the desired density. The following

formula was used to calculate the required volumes of each (2):

$$V_p = V_t \frac{(\rho - 0.1 \rho_{10} - 0.9)}{(\rho_0 - 1)} \quad (16)$$

where  $V_p$  = volume of Percoll required, (mLs)

$V_t$  = total volume desired, (mLs)

$\rho$  = final density desired, (g/mL)

$\rho_{10}$  = density of water, 1.000 g/mL

$\rho_0$  = density of Percoll as supplied by manufacturer, (g/mL)

A total volume of 5 mLs per gradient was found sufficient.

Density ranges exceeding 1.13 g/mL required the concentration of the stock Percoll solution. Concentration by dialysis was used in this research. Several feet of dialysis tubing were boiled for ten minutes in distilled water with a small amount of sodium carbonate. One end of the tubing was tied with plastic clips. The tubing was then filled with Percoll and the free end also tied. The filled tubing was placed in a pan and covered with polyethylene glycol (PEG) flakes. The PEG extracted water through the dialysis tubing to concentrate the Percoll. After several hours, the

tubing was rinsed, and the Percoll removed. The resulting Percoll was a gelatinous substance of unknown density.

The method of density determination required a refractometer and a standard curve relating the density of a mixture of Percoll and water to a refractive index value. Unfortunately, the manufacturer supplied standard curves with only sucrose and salt water as dilution waters. It was necessary to create a standard curve by measuring the refractive index of known densities of Percoll and water. The resulting relationship was linear and is shown in Figure 4. From this plot, the refractive index of concentrated Percoll was measured, and its corresponding density determined.

Having concentrated or diluted the Percoll to cover the necessary range of densities, a method of gradient formation was chosen. The two possibilities explored were manually-layered step gradients and pre-formed, self-generated gradients. In the first method, the densities were prepared individually and carefully layered into a centrifuge tube, in order of decreasing density. A Pasteur pipette was used, keeping the tip on the tube wall just above the liquid surface. Each interface between gradients was marked on the outside of the tube to distinguish between densities after centrifugation.

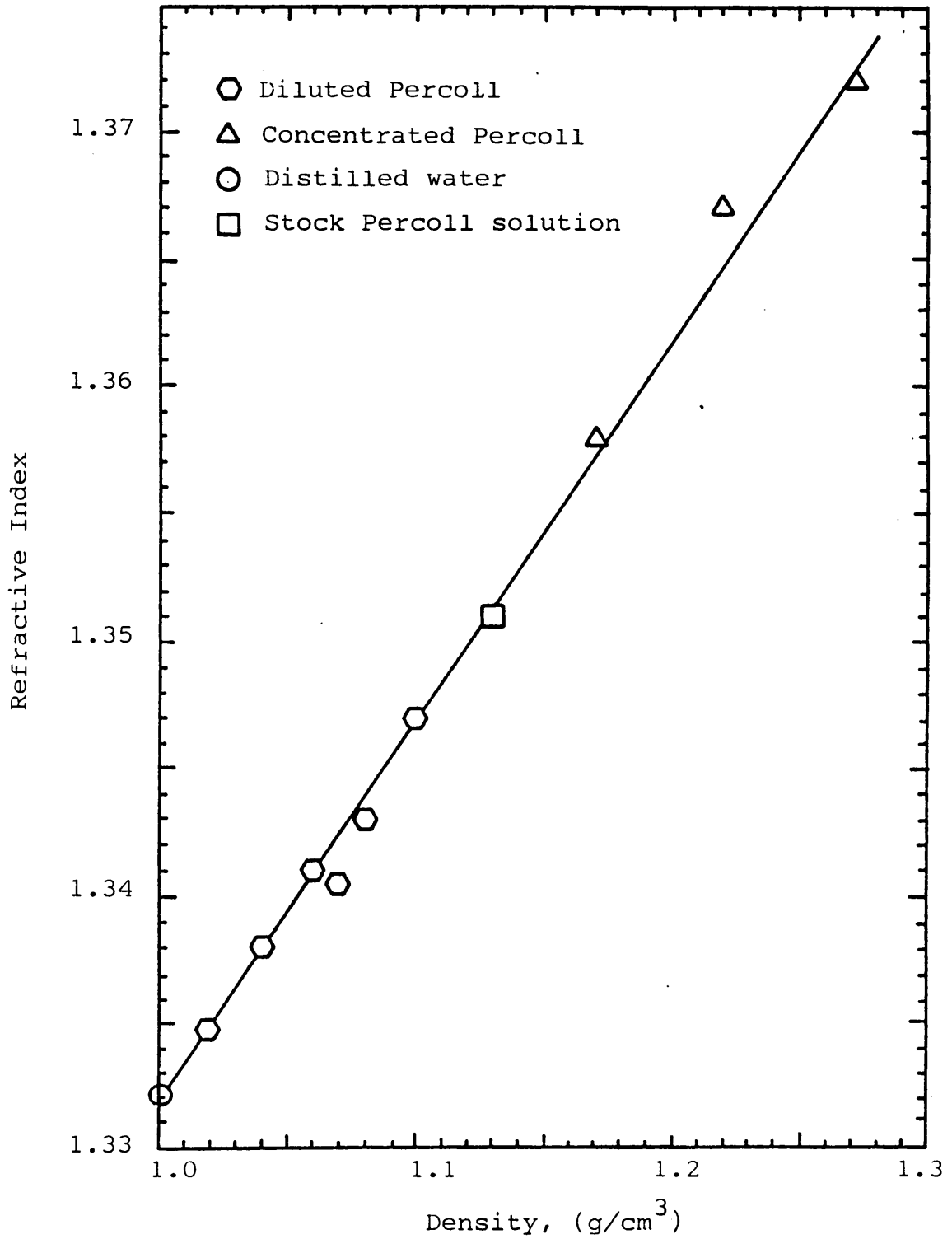


Figure 4: Calibration Curve Relating the Density of Percoll Solutions of Varying Density to Measured Refractive Index, (Temp. = 24.5 °C).



To form self-generated gradients, a density value was chosen in the middle of the desired pre-determined range. A centrifuge tube was filled with Percoll at this density, and self-generated gradients were formed under centrifugation. Although this method was faster, there was no efficient way to measure the resulting density gradients. Density marker beads supplied by the manufacturer were useful only from 1.030 g/mL to 1.093 g/mL. At higher densities, it was necessary to carefully extract Percoll from the gradient of interest and measure its refractive index. This procedure was time-consuming and of questionable accuracy. Therefore, manually layered step-gradients were considered the more efficient method of gradient formation. The improvement of density measurement techniques, especially the development of known density marker beads for higher density ranges, may prove this statement invalid.

Several methods of sample loading were investigated, including top and bottom loading. Samples were also mixed with certain density gradients and layered during gradient formation. Experimental evidence indicated that samples should be top-loaded, with the syringe just breaking the liquid's surface to overcome surface tension. The sample size selected for use was approximately 0.1 mL, or just enough to

form a visible band of sludge particles.

#### Sedimentation Process

Having a centrifuge tube containing gradients and the sample, centrifugation was required to initiate the sedimentation process. For the sludge floc to reach their isopycnic point, consideration of centrifuge type, force and time was necessary. For manually-layered gradients, a swinging-bucket rotor was necessary for sludge banding to occur. For this research, a table-top, swinging-bucket rotor centrifuge was used. If self-generated gradients had been used, an angle-head rotor would have been required.

Time and force of centrifugation were also important. Different combinations were investigated to arrive at optimum values for both. Using hand-layered gradients in a swinging bucket rotor, a centrifugal force of 1,000 g was found adequate to produce discrete floc banding. The time variable was approached by stopping the centrifuge every two minutes and recording the location of the sludge. If the sludge band continued to lower, it had not yet reached its isopycnic point. If its position remained unchanged for four to six minutes, it was considered at equilibrium. In the case of alum sludges, upward movement occurred after approximately eight minutes. It was assumed that sludge floc reached their isopycnic point, then began to

aggregate, producing a lighter density. It became important to monitor the position of the sludge over time intervals to observe its characteristic behavior.

### Floc Density Measurement

Sludge floc showed four reactions to centrifugation in Percoll:

1. Floated - Sludge found floating at the liquid's surface was too light for the chosen density range.
2. Pelleted - Sludge that pelleted to the bottom of the tube was too heavy for the chosen density range.
3. Formed one distinct band - The floc reached its isopycnic point. All floc were of similar density.
4. Formed multiple bands or remained in a scattered suspension - The floc were not of uniform density. The densities where floc came to rest represented the distribution of floc densities within that sludge.

A density measurement was recorded as a single value for a distinct band, or as a range of values for multiple bands or a suspension.

For densities below 1.13 g/mL, the use of density marker beads provided the easiest means of density measurement. The beads were top-loaded with the sample and formed distinct bands at their respective isopycnic points. Each band provided an accurate measure of the density at a particular location.

When density measurements above 1.13 g/mL were necessary, the test-tube demarcations made during gradient formation distinguished between various density bands.

#### IV. RESULTS AND DISCUSSION

The purpose of this section is to present one interpretation of the laboratory data collected in order to gain insight into the behavior of each sludge during thickening and dewatering. By examining test data, specific dewatering characteristics were identified, and a correlation was drawn between these characteristics and fundamental macro- and micro-properties. Two realms of dewatering were investigated: gravity thickening and mechanical dewatering. After dewatering relationships were identified, an attempt was made to construct a physical model that describes changes in the water distribution of sludges as a result of mechanical dewatering.

For each sludge sample, certain fundamental properties were measured or calculated. These values provide key information about any particular sludge. The method of obtaining each parameter is listed in Table 2, along with relevant calculation equations. Also, a summary of calculated values for the sludges tested is provided in Table 3. This table will be referenced throughout the following discussion sections.

**TABLE 2**  
**Methods of Determination For Various Fundamental  
 Sludge Properties**

Property	Symbol	Method of Determination	Equation
Floc Density (g/mL)	$\rho_f$	Direct measurement by density gradient centrifugation	-
Dry Density (g/mL)	$\rho_k$	Calculation	(1)
Aggregate Density (g/mL)	$\rho_a$	Calculation	(2)
Bulk Density (g/mL)	$\rho_b$	Direct measurement with pycnometer	(11)
Dry Solids Conc. (%)	%SS	Oven drying method of direct measurement	(12)

TABLE 3  
Calculated Values of Various Fundamental Sludge  
Micro-Properties

Sludge Type	Floc Density (g/mL)	Aggregate Density (g/mL)	Dry Density (g/mL)
Ferric	1.11	1.001	2.47
Unc Alum	1.15-1.18	1.010	2.61
Cond Alum	1.17-1.20	1.021	2.49
Lime	1.50 (estimated)	1.070	2.12

### Gravity Thickening

Gravity thickening of sludges was simulated using batch settling tests as described in Chapter III. From direct measurement, graphical analysis and calculation, four sludge parameters were produced which describe particle characteristics during settling.

#### Bulk Density

The bulk density of gravity thickened sludge solids was measured directly. As shown in Table 4, for three of the four sludge samples, the thickened sludge bulk density was greater than calculated values for aggregate density (based on equations provided by Javaheri and Dick (7)). In most cases, the two values were nearly identical. This occurrence might be explained by recalling the model of differential settling zones. In the compression phase of thickening, particles are squeezed by the overlying weight of supernatant and sludge. If aggregates were compressed, then  $\rho_b$  of the thickened solids should have been greater than the calculated  $\rho_a$ . A comparison reveals  $\rho_b \geq \rho_a$  for all four sludges, lending evidence to the theory that gravity thickened solids were composed of compressed aggregates.



**TABLE 4**  
**Properties of Sludges After Gravity Thickening**

Sludge Type	Thickened Solids Conc. (g/L)	$\rho_b$ (g/L)	$\rho_a$ (g/L)	$V_o$ (m/hr)	AVI
Ferric	4.6	1003	1001	7.7	1380
Unc Alum	30.0	1017	1010	5.3	164
Cond Alum	35.0	1020	1021	4.3	70
Lime	315.0	1231	1070	2.5	16
Pure CaCO <sub>3</sub> (17)	-	-	-	1.3	2.1
Glass Beads (17)	-	-	-	4.9	1.1

### Settling Velocities and the Aggregate Volume Index

From the raw data collected, a plot was made of interface height versus time of settling for each sludge. For the purpose of illustration, the data for unconditioned alum sludge samples are presented in Figure 5; data for the remaining sludges are provided in Appendix A. As shown in Figure 5, the data plot as a straight line for a period of time. This linear portion of the graph describes the period of zone settling. The slope of this line yields the settling velocity for a certain sludge at a specific initial dry solids concentration.

At this point, two samples were introduced from the literature (17) to offer more data for comparison. The first sample was a pure calcium carbonate ( $\text{CaCO}_3$ ) slurry with  $\rho_k = 2.69$  g/ml. The second was a slurry of glass beads with  $\rho_k = 2.50$  g/ml. Dry solids concentrations and corresponding settling velocities were developed from data provided by Javaheri (17).

For each of the six sludges,  $\phi_k$  values were calculated for a given  $V_s$  and dry solids concentration. A plot of  $V_s^{1/4.65}$  versus  $\phi_k$  was made in an effort to determine the appropriate AVI and  $V_o$  values for each sludge. The data for unconditioned alum are presented in Figure 6, for illustrative purposes. For purposes of calculation and comparison, one AVI value was recorded for each sample, based upon data taken only from the

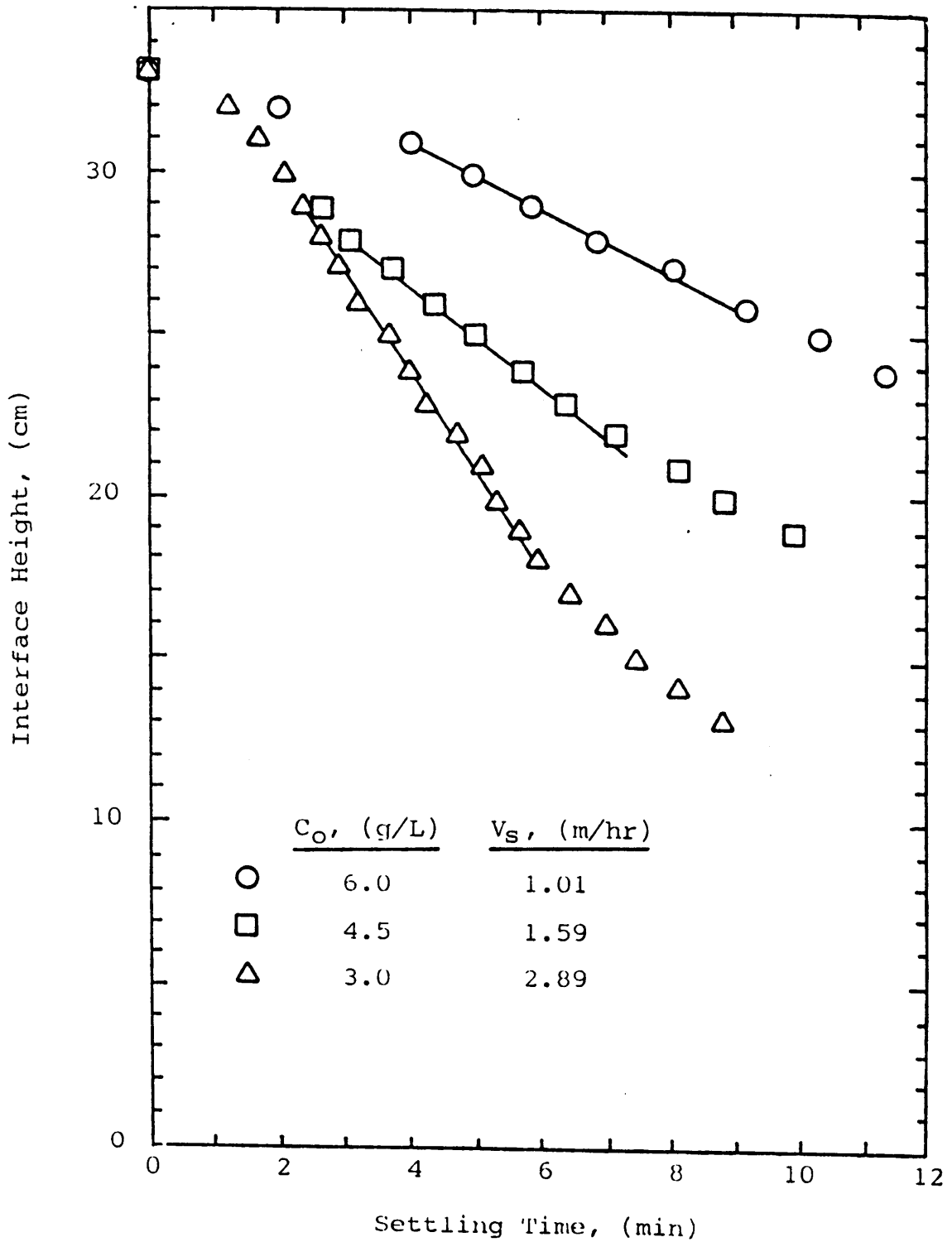


Figure 5: Determination of Zone Settling Velocities at Various Concentrations of Unconditioned Alum Sludge.

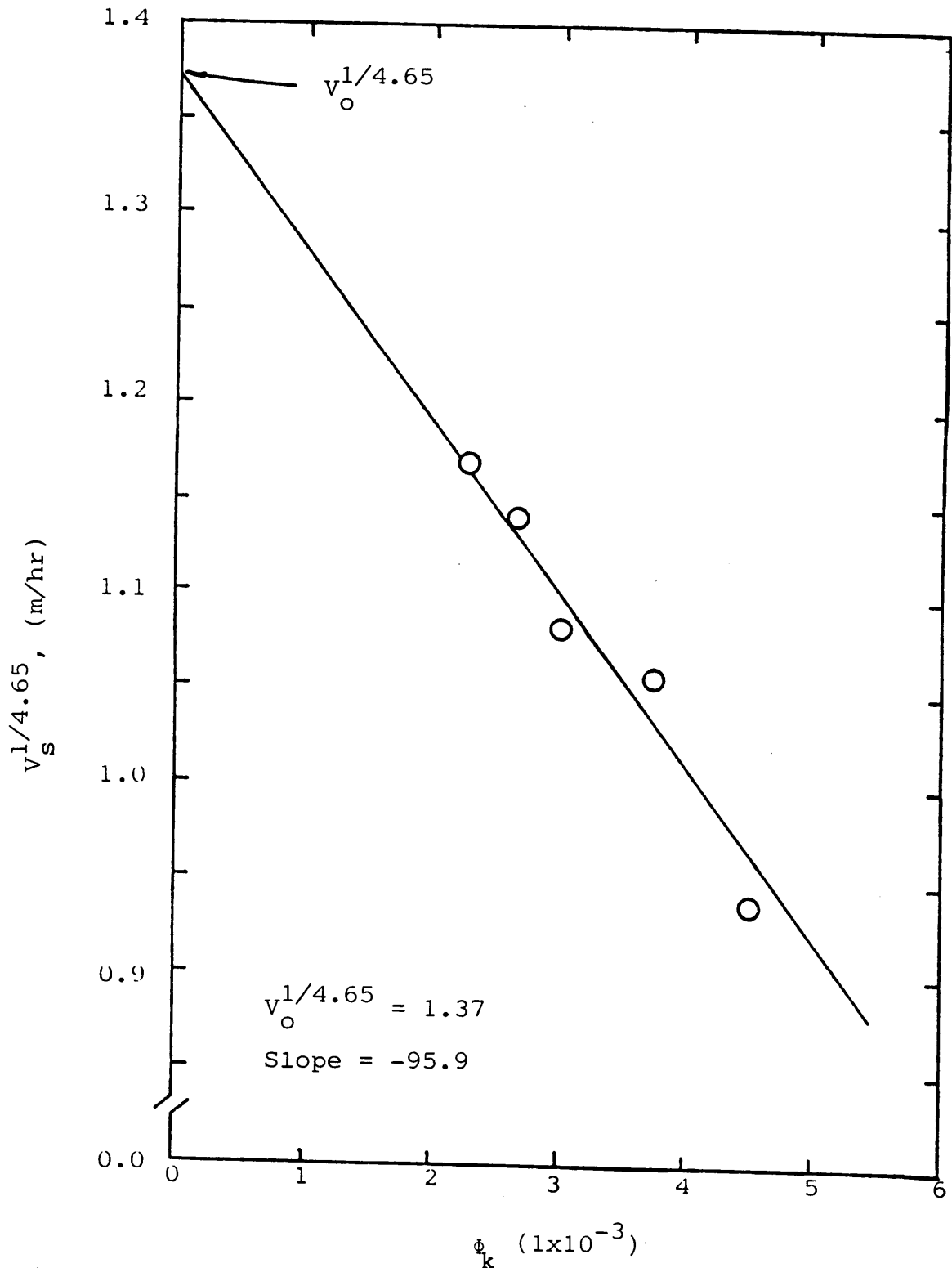


Figure 6 : Relationship Between Zone Settling Velocity and Volume Fraction of Dry Solids for Conditioned Alum sludge.

zone settling stage of thickening, where aggregate structure was considered undeformed by compression. The same assumption applied when determining  $V_0$ . Both parameters are presented in Table 4 for each sludge.

Interpretation of the preceding parameters led to the following sludge characterization: Ferric sludge contained the largest, lightest aggregates with the corresponding highest water content. In comparison, the unconditioned alum sludge had a much reduced apparent water content. Polymer addition lowered the alum sludge water content significantly, thereby increasing the apparent aggregate density.

Of the four laboratory sludges tested, lime had the smallest and most dense aggregates. Pure  $\text{CaCO}_3$  appeared to have the smallest aggregate size of all six samples. A very low aggregate water content was also suggested by the low AVI value for this sludge. Finally, the glass beads, of intermediate aggregate size, contained almost no water. Theoretically, the minimum AVI value is 1.0, the case when the entire aggregate is composed purely of dry solids. The AVI value of approximately 1.1 for glass beads suggests that the aggregate volume of the glass beads was nearly equivalent to the volume fraction occupied by the dry bead material. It is important to note the extremely close agreement between the experimen-

tally determined AVI for the glass beads and the theoretical AVI. This result helps to validate the hypothesis that the AVI may be used as a reliable, comparative measure of aggregate water content.

By analyzing the plots of  $(V_s^{1/4.65})$  versus  $\phi_k$  for each sludge, certain comments can be made about aggregate behavior during settling. According to Javaheri and Dick (7), a linear plot indicates unchanging  $V_o$  and AVI values. For some sludges, though, the plot of  $(V_s^{1/4.65})$  versus  $\phi_k$  is curved, indicating a significant change in aggregate size and a release in water content during thickening. This behavior was especially evident when considering the lime thickening data. By applying ideas from the literature (7), one may conclude that thickened lime aggregates contained less water and were of smaller diameter than unthickened lime aggregates. This behavior is typical of a sludge being compressed by the weight of overlying solids and supernatant.

The traditional plot of  $\log(V_s)$  versus initial dry solids concentration was made to compare settling characteristics among the six sludges (Figure 7). A sludge exhibiting the least variation in  $V_s$  with respect to mass solids concentration is most desirable, as this helps to maximize solids flux through a gravity thickener. Note the difference in scales on the two horizontal axes. The plots for ferric and alum sludges are almost

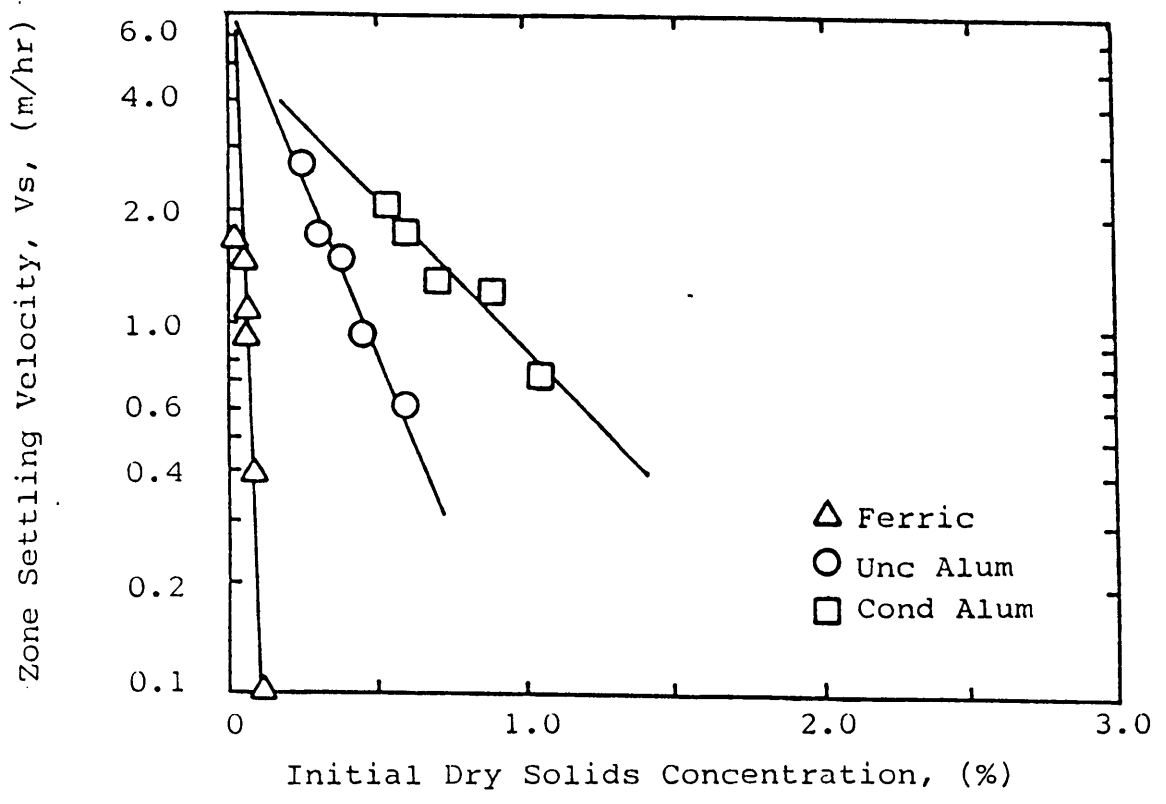
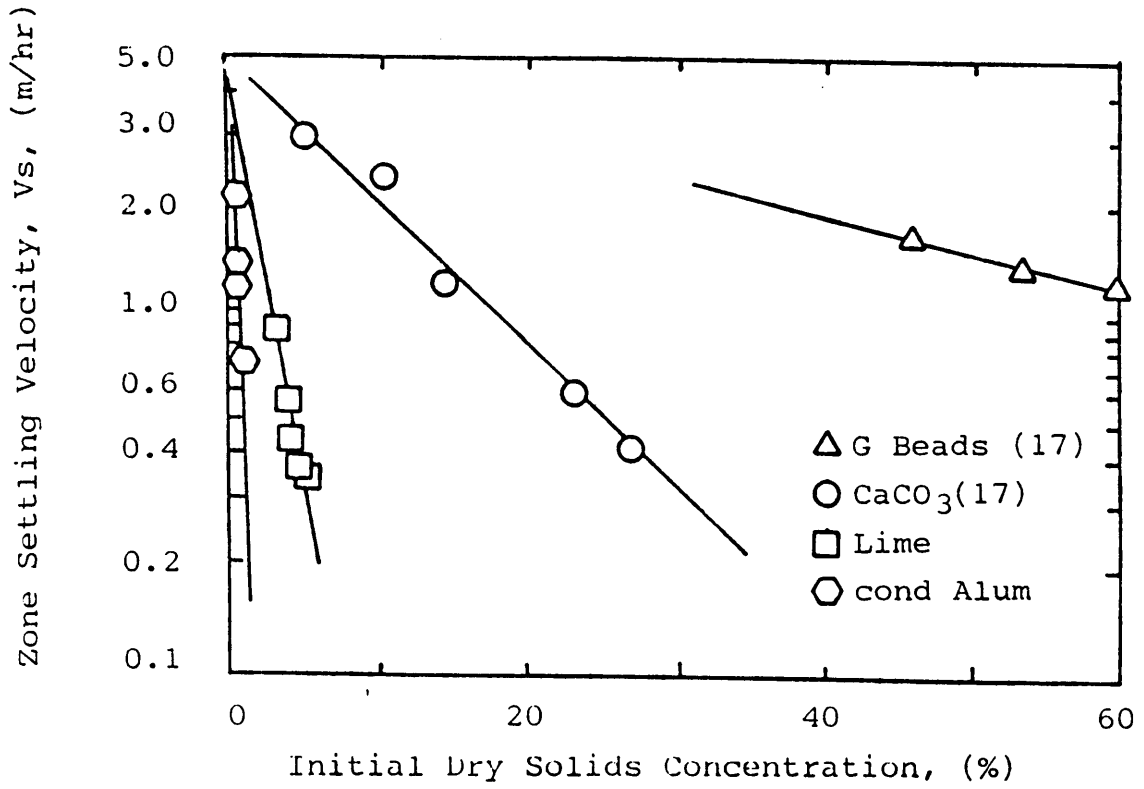


Figure 7: Relationship of Zone Settling Velocity and Dry Mass Solids Concentration for Six Sludges.

vertical in comparison to the lime, pure  $\text{CaCO}_3$ , and glass beads, indicating a greater change in settling behavior for a given change in dry solids concentration. The glass beads and pure  $\text{CaCO}_3$  demonstrated nearly ideal thickening characteristics, i.e., almost no change in zone settling velocity with respect to an increase in mass solids concentration. Lime sludge exhibited the least variation of the four chemical sludges tested, followed by conditioned alum, unconditioned alum, and ferric sludge, respectively.

Analysis of the data presented in Figure 7 yields the following observations:

(1.) For any given sample, an increase in mass solids concentration caused the zone settling velocity or thickening rate to decrease. Higher sludge concentrations resulted in decreased suspension porosity. As cited previously, Richardson and Zaki (8) showed that sludge thickening rates were significantly impacted by a change in porosity (Equation 7). This change in porosity produces a significant increase in surface drag resistance as water moves upward through the sludge aggregates. Consequently, sludges with higher mass solids concentrations thicken at slower rates.

(2.) Figure 7 did not reveal a significant pattern between sludge settling velocity and dry mass solids concentration. In search of a parameter bearing direct



influence on settling characteristics, the plots in Figure 7 were transferred to plots of settling velocity versus volume fraction occupied by sludge aggregates. A comparison of sludge settling characteristics on a volume basis served to remove the density factor. From Equation 4, at a given mass solids concentration, a lighter sludge should occupy more space. Thus, when two sludges of unequal density are compared on a mass solids concentration basis, the denser sludge occupies less volume. By removing density considerations, it was revealed that a significant relationship exists between settling velocity and corresponding aggregate volume fraction. Figure 8 shows a remarkable similarity in settling characteristics among all six sludges. The nearly parallel lines indicate that sludges of unequal densities responded in nearly an identical way to changes in aggregate volume. A similar plot was constructed by Knocke (10) using activated sludge data. The results showed that nearly parallel lines were obtained when the sludges were compared on a volume basis.

Calculated mathematical expressions for the lines in Figure 7, equations were generated of the form:

$$V_s = V_o 10^{-kc} \quad (17)$$

These equations are recorded in Table 5 for each sludge

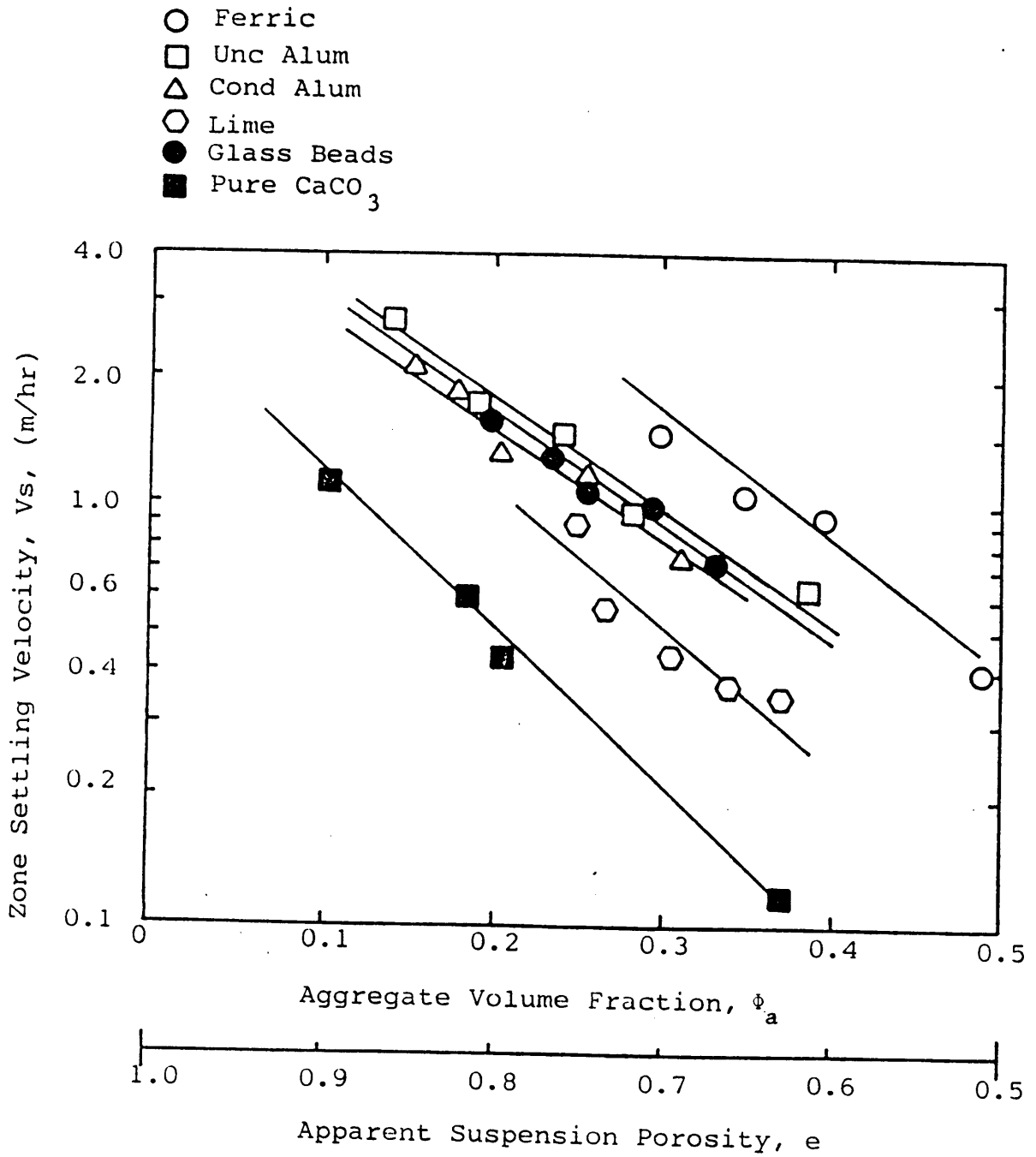


Figure 8: Relationship of Zone Settling Velocity and Sludge Aggregate Volume Fraction for the Six Sludges Examined in this Study.

TABLE 5

Equations Relating Interface Settling Velocities to  
Initial Dry Solids Concentration from Figure 7

Sludge Type	Equations of the form $V_s = V_0 10^{-kc}$
Ferric	$V_s = 9.51 \times 10^{-16.5c}$
Unconditioned Alum	$V_s = 6.73 \times 10^{-1.8c}$
Conditioned Alum	$V_s = 5.60 \times 10^{-0.8c}$
Lime	$V_s = 4.76 \times 10^{-0.24c}$
Pure $\text{CaCO}_3$	$V_s = 5.06 \times 10^{-0.04c}$
Glass Beads	$V_s = 4.83 \times 10^{-0.01c}$

type. The  $k$  value represents the slope of each line. A plot of  $k$  versus AVI for each sludge type is presented in Figure 9. As Knocke emphasized (10), a sludge's aggregate water content was seen to influence its settling velocity.

Similarly, equations were derived for the data in Figure 8, of the form:

$$V_s = V_o 10^{-k\phi_a} \quad (18)$$

These equations are recorded in Table 6 for each sludge type. By combining data from this research with that from literature studies (10), the  $k$  values were found to equal approximately 3.0, when making comparisons on a volume fraction basis. No explanation has been developed to explain why  $k$  equals 3.0.

Further analysis of the data in Figure 8 reveals a significant relationship between  $V_s$  and particle size. For a given  $\phi_a$ , settling velocities were greater for sludges containing larger particles (as quantified by comparing apparent Stokes' Law settling velocities,  $V_o$ ).

The significance of porosity will now be discussed in connection with sludge settling characteristics. The aggregate volume fraction has been established as an influential parameter for determining settling velocity.

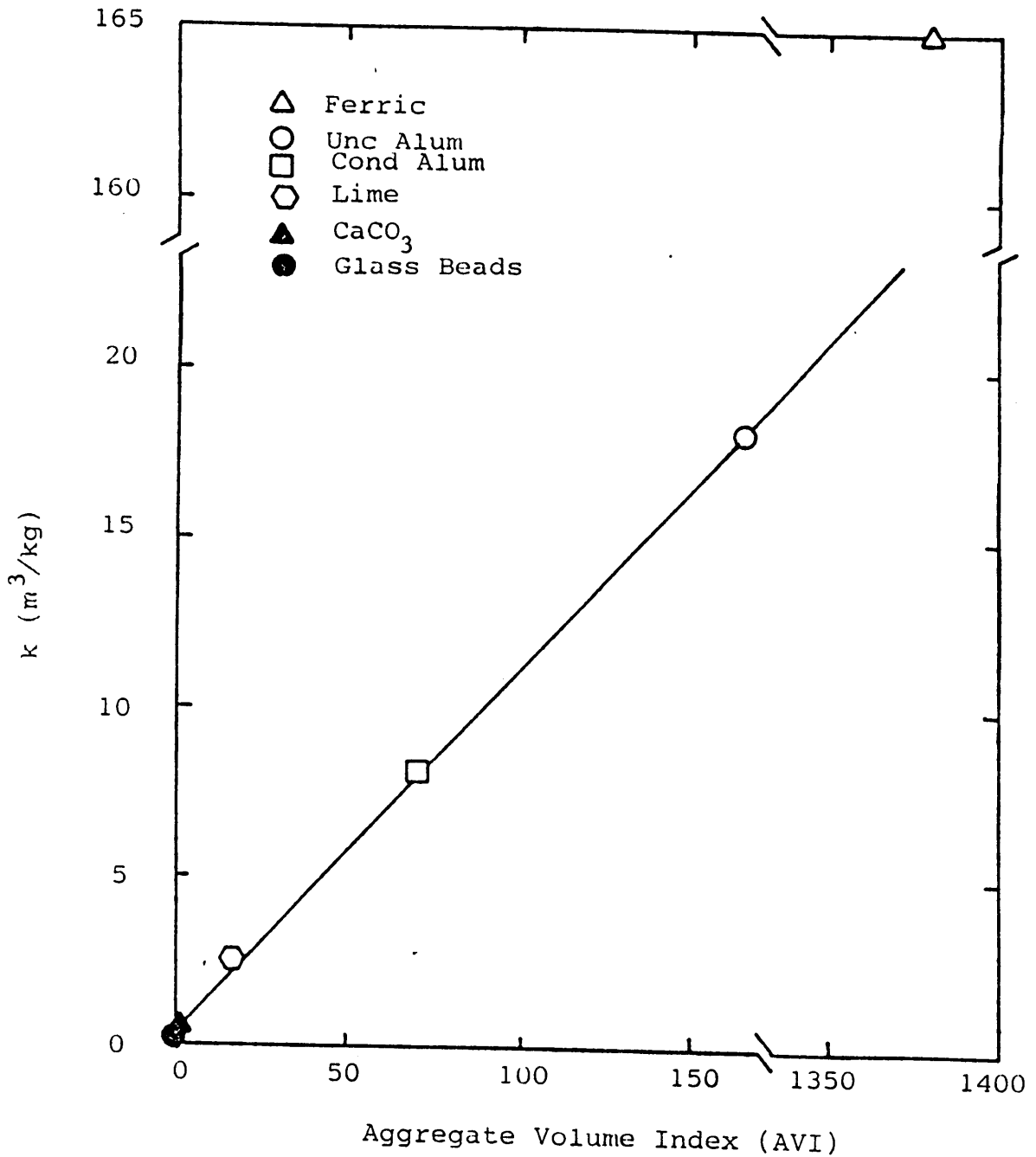


Figure 9: Observed Experimental Data Relating Thickening Constant (k) to the Aggregate Volume Index.

TABLE 6

Equations Relating Interface Settling Velocities to  
Aggregate Volume Index from Figure 8

Sludge Type	Equations of the form $V_s = V_o 10^{-k\phi_a}$
Ferric	$V_s = 13.8 \times 10^{-3.05\phi_a}$
Unconditioned Alum	$V_s = 6.4 \times 10^{-2.74\phi_a}$
Conditioned Alum	$V_s = 6.8 \times 10^{-3.02\phi_a}$
Lime	$V_s = 4.5 \times 10^{-3.12\phi_a}$
Pure $\text{CaCO}_3$	$V_s = 2.9 \times 10^{-3.75\phi_a}$
Glass Beads	$V_s = 6.4 \times 10^{-2.84\phi_a}$

Specific reasons for this influence are related to sludge porosity. According to Javaheri and Dick (7), the porosity of a sludge suspension ( $e$ ) is comprised of the interstices between the aggregates. In mathematical terms:

$$e = (1 - \phi_a) \quad (19)$$

From Equation 19,  $\phi_a$  and  $e$  are inversely related, i.e., in a sludge of high porosity, the amount of volume occupied by aggregates will be comparatively small. Examination of Figure 8 leads to the conclusion that when settling velocities were high, porosity was also high. Similarly, lower velocities were associated with lower suspension porosities. The explanation lies in the resistance to fluid flow caused by surface drag forces. Higher porosities are associated with low aggregate volume fractions and corresponding low surface areas. With less surface area to cause hindering drag forces, the fluid is more easily displaced around the aggregate. This low resistance leads to faster settling of sludge aggregates. The previous discussion provides a possible explanation for the statement by Javaheri and Dick (7) that high porosities are associated with good sludge settling characteristics. A specific example is provided by comparing the porosities of unconditioned

alum and lime at a mass solids concentration of 1%.

Using Equation 19:

$$\text{unconditioned alum: } e = 1 - (0.628) = 0.372$$

$$\text{lime: } e = 1 - (0.075) = 0.925$$

The lower settling velocity of unconditioned alum at 1% mass solids concentration could be explained by its significantly lower porosity, which contributed to higher surface drag forces.

In summary, several important micro-properties were discussed that could significantly influence sludge thickening characteristics. A summary of each term's relationship to the observed rate and extent of sludge thickening is provided in Table 7.

### Mechanical Dewatering

Mechanical dewatering was performed by vacuum filtration, centrifugation, and high-pressure dewatering techniques. Using data from these three methods, the study of sludge behavior during dewatering was undertaken. First, certain relationships were analyzed. Second, specific parameters were calculated and evaluated for their influence on the extent of dewatering. Finally, changes in particulate structure were noted.

### Important Sludge Relationships

A plot of solids concentration versus applied



TABLE 7

Summary of Relationships Between Important Sludge  
Micro-Properties and Corresponding Sludge  
Thickening Characteristics

An increase in	Results in a(n)
$\phi_a$	decrease in $V_s$
$\rho_a$ , at a given mass solids concentration	increase in $V_s$
$e$ , at a given mass solids concentration	increase in $V_s$
particle size, at a given $\phi_a$	increase in $V_s$
apparent aggregate water content (quantified by AVI)	decrease in suspended solids conc. after gravity thickening

mechanical pressure was made and is shown in Figure 10. The maximum pressure applied by vacuum dewatering was approximately 0.5 bars. Data for high-pressure dewatering were collected at 1 bar, 3 bars, and 15 bars of pressure. Figure 10 reveals that the four chemical sludges reacted similarly to applied pressure. Specifically, most water was removed at lower pressures. The extent of dewatering observed increased at higher applied pressure differentials until the sludges reached a steady-state moisture content, indicated by the almost unchanging solids concentrations observed when comparing dewatering results for both the 3 bar and 15 bar pressures.

Certain hypotheses were made by comparing bulk density to dry solids concentration. A plot was made for each sludge that related these parameters through various phases of dewatering: from gravity thickening, through mechanical dewatering, to high-pressure methods. The plots are presented in Figures 11 through 13 for ferric, alum and lime sludges. Since results for conditioned and unconditioned alum differed only slightly, these data were combined. The plots illustrate an apparent linear relationship between the two parameters. However, if each curve were extrapolated to a 100% dry solids concentration, the corresponding bulk density would not equal the calculated dry density of each

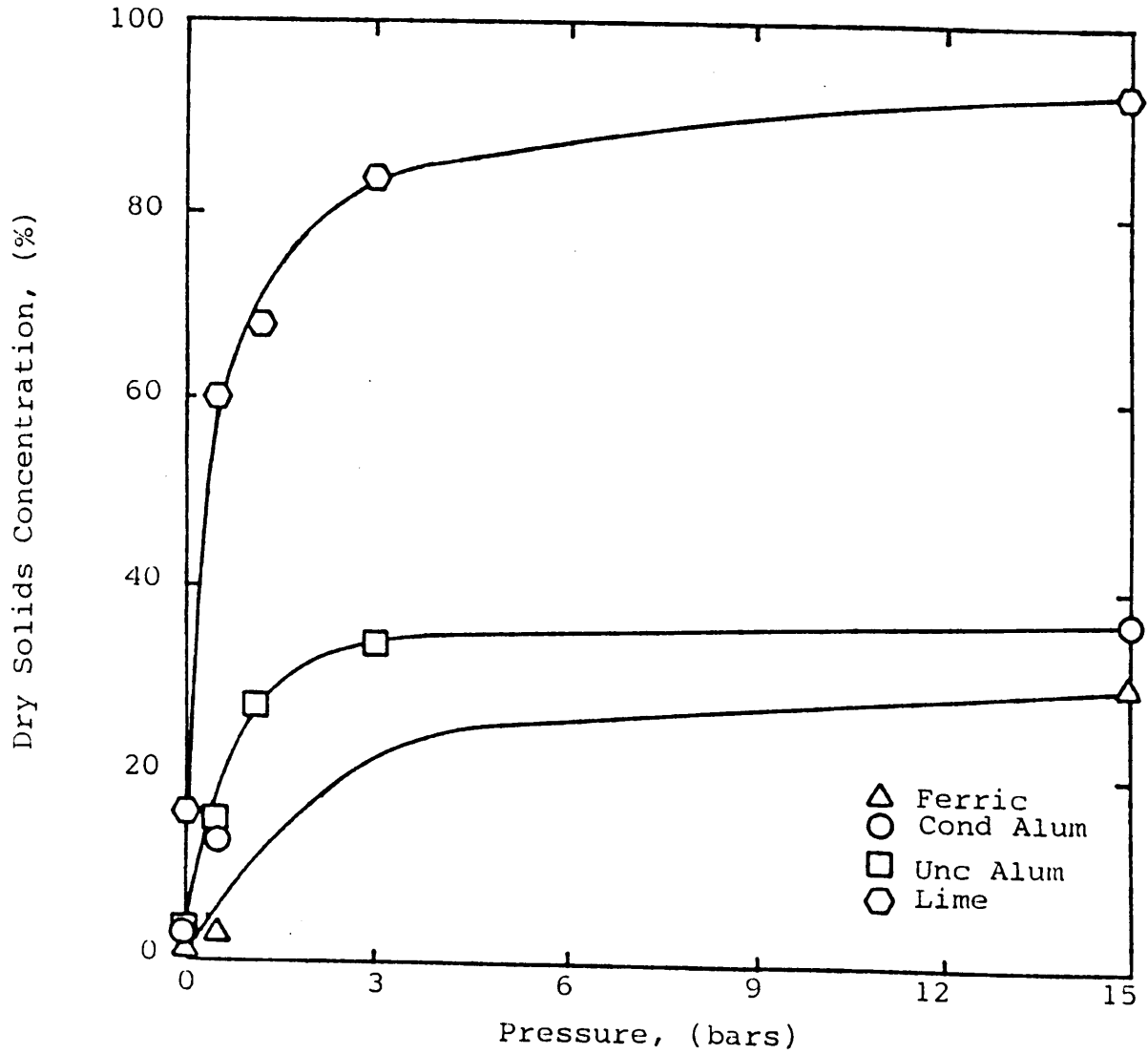


Figure 10: Effect of Applied Pressure on the Extent of Sludge Dewatering Observed.

sludge. One possible explanation for this contradiction is that the relationship is linear only for a certain range of solids concentrations; at higher concentrations, the curve may become more vertical to approach its dry density at 100% dry solids concentration. A second possibility is that the method of calculation for sludge dry density (Equation 1) is incorrect. If the latter is true, the results of this research are not invalidated. The calculation of AVI and  $\phi$  would be slightly lowered. In either case, it is acknowledged that a contradiction exists between laboratory and graphical data. However, Figures 11, 12, and 13 still yield a number of interesting observations.

1. The plots illustrate the potential for water release during the compression phase of gravity thickening, as indicated by instances where thickened bulk densities equaled or exceeded calculated aggregate densities.

2. Similar results were obtained from using the centrifuge and the Buchner funnel apparatus. The maximum bulk densities reached by both types of equipment exceeded aggregate densities but did not exceed measured floc densities. One interpretation of these results is that during mechanical dewatering by centrifugation and vacuum filtration, aggregate structure was destroyed, while floc structure was

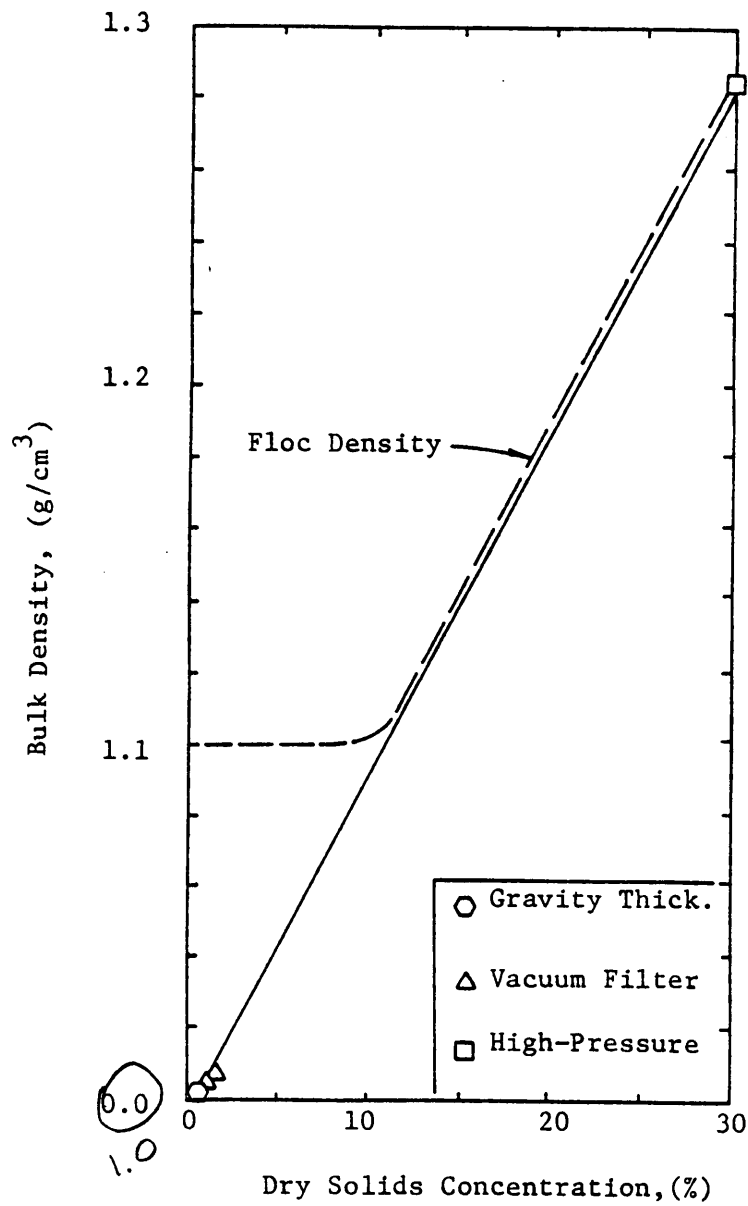


Figure 11: Relationship Between Measured Bulk Density and Dry Solids Concentration During the Dewatering of Ferric Hydroxide Sludge.

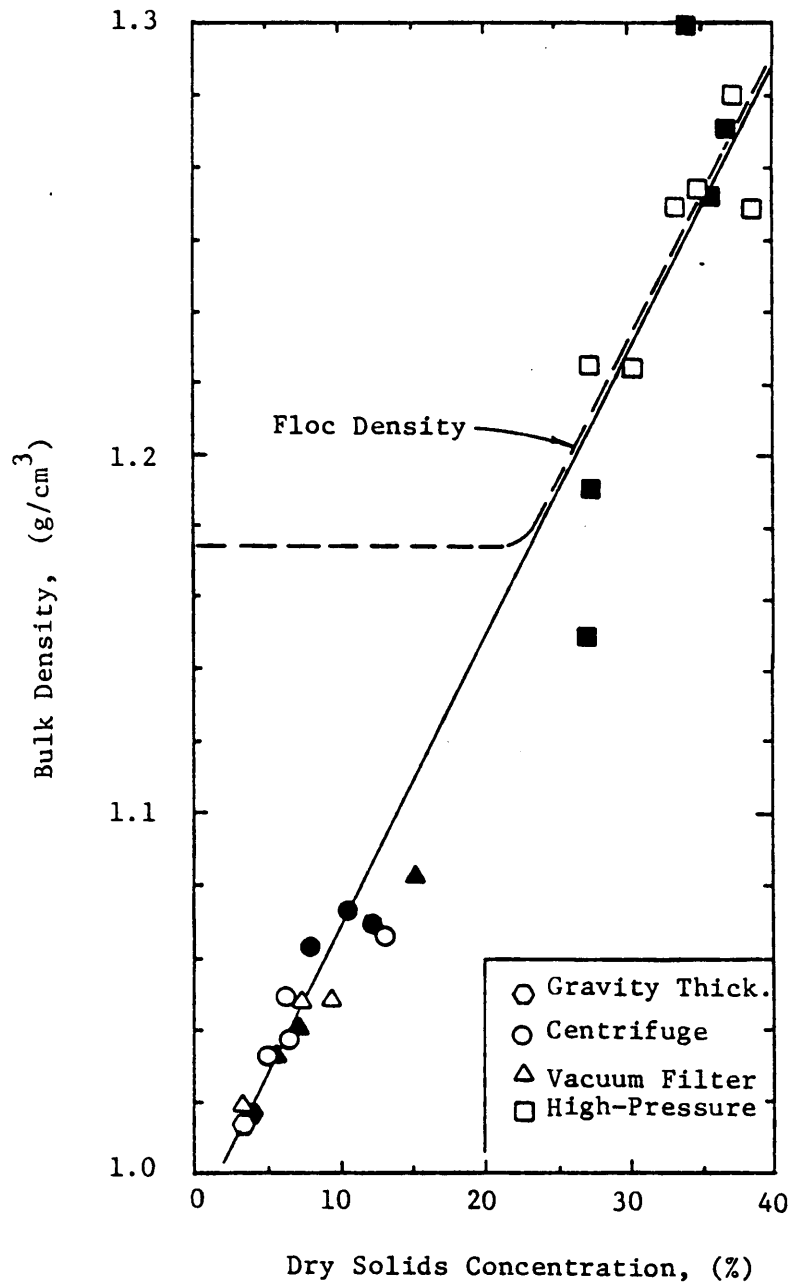


Figure 12: Relationship Between Measured Bulk Density and Dry Solids Concentration During the Dewatering of Unconditioned Alum (open symbols) and Conditioned Alum (closed symbols) Sludges.

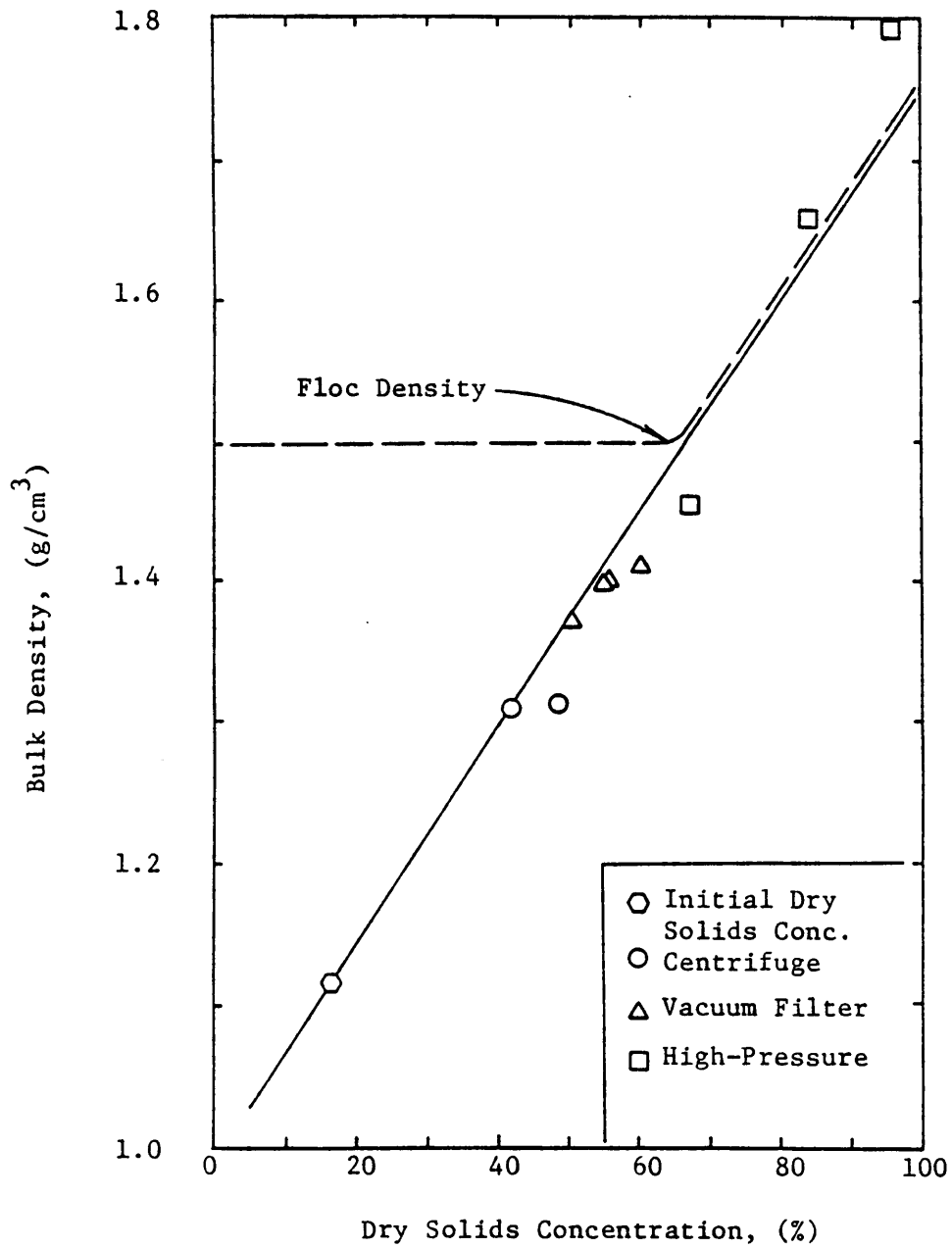


Figure 13: Relationship Between Measured Bulk Density and Dry Solids Concentration During the Dewatering of Lime Sludge.

maintained.

3. Bulk densities appeared to exceed measured floc densities only during high-pressure dewatering. According to the following mass balance:

$$\rho_b = \phi_f \rho_f + (1 - \phi_f) \rho_w \quad (20)$$

A bulk density measurement is calculated by adding proportional fractions of floc density and the density of the interfloc water. Thus, bulk density measurements should be less or equal to than floc density measurements. The fact that bulk densities exceeded measured floc densities at high pressures could be interpreted as the initiation of floc deformation. If the floc matrix was pressurized to release internal water, the floc density would increase. For this reason, the dashed floc density lines were included in Figures 11 and 12. Before deformation, floc structure would be intact and would maintain a constant density. If pressures became great enough to remove water from the internal floc structure, floc density would increase accordingly.

Given the preceding premise, the break-down of floc structure was felt to occur during the early stages of high-pressure dewatering. By examining the dewatering characteristics of ferric and alum sludges, the floc density of lime sludge may be estimated. The measured floc densities



of ferric and alum sludges correspond to a pressure of 1 bar (Figure 10). Assuming that lime sludge behaved similarly, the floc density of lime was estimated as the bulk density at 1 bar pressure, corresponding to a density of approximately 1.5 g/mL. This information was obtained from Figures 10 and 13. Thus, for future calculations, 1.5 g/mL is used as the estimated floc density of lime sludge. It should be noted that this approximation method, although hypothetically based, was necessary to attempt a comparative interpretation of the lime sludge data. All centrifugal density determinations on the lime sludge floc resulted in sludge pelleting in the bottom of the centrifuge tube. Given that Percoll, with a density as high as 1.3 g/mL, was used in these tests, these results would indicate that the lime floc density was well in excess of 1.3 g/mL.

4. For each sludge, the maximum dewatered bulk density measurement remained below the calculated value for dry density. This fact reinforces the concept that even high-pressure dewatering cannot remove all traces of sludge moisture. The water remaining might be classified as representing, to a significant extent, the chemically bound water fraction.

#### Parameters Affecting the Extent of Dewatering

Past studies emphasized the analysis of dewatering rates. A second practical concern is the extent of

dewatering achieved by a given sludge using specific dewatering equipment. According to a current EPA Design Manual (15), maximum performance capabilities of centrifugation and vacuum filtration range from 22-32% solids for various biological sludges. High-pressure equipment, such as a plate-and-frame filter press, were able to attain up to 50% dry solids concentration with digested primary sludge. From this information, laboratory vacuum dewatering and centrifugation methods were compared with vacuum filtration and centrifugation processes in practice. Similarly, laboratory pressure plate tests were considered analogous to filter press dewatering methods.

The extent of sludge dewatering is typically reported as a mass solids concentration. However, this value does not allow an accurate comparison among sludges with varied properties. As discussed earlier, sludges possess different densities which dictate the volume of sludge present at a given mass solids concentration. A valid comparison must remove the density factor in order to adequately analyze the sludges. For this reason, floc volume fractions were used to investigate the extent of dewatering achieved by different sludges.

Floc volume fractions and corresponding solids concentrations were calculated at two points during

dewatering. The first point represented the maximum dewatering capability of the centrifuge and Buchner funnel apparatus. The second point corresponded to the limit of mechanical dewatering, or 15 bars. These values are shown in Table 8.

The data revealed a direct correlation between the extent of dewatering and the volume occupied by sludge floc. Lime sludge showed significantly greater dewatering abilities than the other three samples. The ultimate solids concentration reached at both specified points was well above that of alum or ferric sludge. Considering  $\phi_f$ , the lime flocs occupied over half the total cake volume, while the lesser dewatered sludges achieved maximum floc volumes of under 30%.

By comparing the four sludges on a floc volume basis, it is clear that the greatest extent of dewatering is associated with a sludge cake of high floc volume. Although this statement appears simple, its application provides insight into mechanical dewatering processes. Drawing upon the aforementioned analogies between laboratory and applied dewatering techniques, equipment efficiency appears to be a function of floc volume. The higher efficiency of the filter press is attributed to its ability to achieve greater floc volume fractions in the dewatered sludge.

Particulate Structure Changes during Dewatering

TABLE 8

Calculation of  $\phi_f$  For Corresponding %SS at Two Stages  
of Mechanical Dewatering

Sludge Type	Max %SS from C & VD	$\phi_f$ from C & VD	Extent of MD, (%)	$\phi_f$ at extent of MD
Ferric	3.1	0.03	30.2	0.24
Unc Alum	13.2	0.11	37.7	0.29
Cond Alum	15.2	0.13	36.3	0.28
Lime	60.1	0.40	92.6	0.55

C = Centrifuge  
VD = Vacuum Dewatering  
MD = Mechanical Dewatering

Information from gravity thickening studies was combined with dewatering results to form a theoretical model of floc changes during dewatering. Batch thickening tests began with a hydrated aggregate that released free water through hindered settling. If this aggregate entered a zone of compression, overlying pressure could cause the removal of internal aggregate water. Thus, gravity thickening solids could be composed of dehydrated aggregates with deformed structures.

As seen from Figures 11, 12, and 13, densities from centrifugation and vacuum dewatering never reached floc density measurements; floc density was considered unaffected by these dewatering methods. Water removal in both dewatering methods was felt to come from outside the floc structure with little or no internal floc water release. The species resulting from centrifuge and vacuum dewatering could be a hydrated, undeformed floc.

During the early stages of high-pressure dewatering, bulk densities exceeded floc densities. This fact was interpreted to signify the initiation of floc structure deformation. As dewatering continued, the sludge reached a steady-state moisture content, indicated by the negligible change in solids concentrations between 3 bars and 15 bars.

#### A Model of Water Distribution

The relative distribution of dry matter and water

within a sludge depends upon physical and chemical forces that bind the water to the dry sludge. These forces are important, not only in developing a theory of water distribution, but in putting that theory to practical use. If forces are better understood, then dewatering methods can be improved to attack specific binding forces and promote more efficient water removal techniques.

The description of water distribution qualifies and quantifies the water in a sludge. In this section, the theory was discussed in terms of sludge parameters and observations made during phases of dewatering.

This research recognized four categories of water. Each type was defined by its corresponding dewatering method. Again, these definitions represent one interpretation of the laboratory data. Following the qualification of the water types, water distribution was quantified for specific sludges tested.

Interspace/free water. This category refers to loosely bound, interaggregate water. Its quantity can be estimated by measuring the water removed during gravity thickening. The fact was noted that the bulk density of gravity thickened solids varied slightly from aggregate density measurements. Since the differences were small, the sludge from gravity thickening was assumed to be in aggregate form. Therefore, the water

removed during gravity thickening was considered free, or interspace water.

Interfloc/intra-aggregate water. This category defines water that was enclosed in the aggregate structure, but remained outside the floc structure. The force binding the water to the sludge was the force of interlocking floc which combine to form aggregates. When these floc were disrupted, the water was freed.

Mechanical dewatering produced sludges with densities below measured floc values, but exceeding aggregate densities. Apparently, aggregate structures were disrupted during mechanical dewatering, while floc structures remained intact. This concept differs from Vesilind's, which argued that sludge floc were deformed during centrifugation. Vesilind expected to see a sudden break in a plot of solids concentration versus centrifugal acceleration. This break would represent a great water release, indicative of floc structure deformation. As shown in Figure 14, however, the observed relationships were relatively smooth, signifying no floc structure deformation took place. This observation was reinforced by data presented by Wakeland (16). Thus, Vesilind's theory that internal floc water is released during centrifugation may be considered questionable.

To summarize, interfloc/intra-aggregate water is

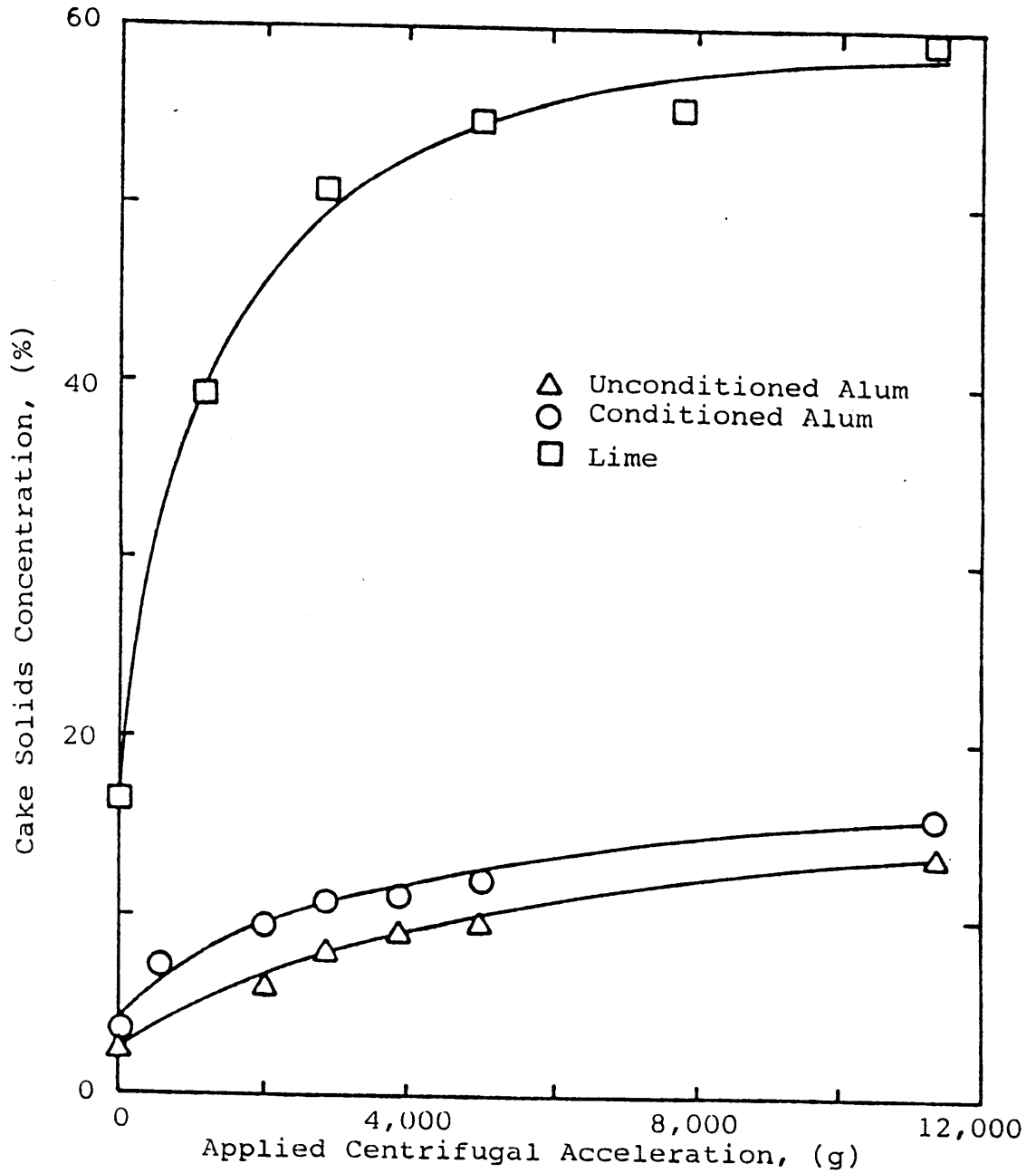


Figure 14: Effect of Centrifugal Acceleration on Extent of Sludge Dewatering Observed.



that fluid removed after the break-down of aggregate structure, but before the deformation of floc structure. In terms of dewatering procedures, this water-type was removed by centrifugation and vacuum dewatering, and during the early stages of high-pressure dewatering.

Intrafloc water. Intrafloc water is that fluid found within the floc particle. Its removal was accomplished with a high-pressure dewatering technique. Intrafloc water removal began after floc deformation and continued through maximum mechanical dewatering pressures.

Adsorbed and internal water. Observed data indicated that not all water was removed by the laboratory dewatering procedures used. Specifically, after a pressure of 15 bars was applied, each sludge maintained a certain level of moisture. This statement was supported by Figure 10 where, at 15 bars of pressure, the increase in solids concentration was almost negligible. At this point, dewatering by mechanical means was considered exhausted. The remaining moisture was termed "adsorbed and internal water." Möller (14) described this fluid as particle moisture and chemically bound water that can only be removed by destroying the particle structure or by transforming internal water into external water.

The quantification of sludge water-types was best approached by comparing relative volumes of aggregates and floc during dewatering. Four descriptive parameters

were calculated for each sludge using the following mass balances:

$$(1) \rho_b = \phi_a \rho_a + (1 - \phi_a) \rho_w \quad (22)$$

$$(1) \rho_b = \phi_f \rho_f + (1 - \phi_f) \rho_w \quad (23)$$

$$(1) \rho_b = \phi_{f'} \rho_{f'} + (1 - \phi_{f'}) \rho_w \quad (24)$$

where  $\rho_{f'}$  represents the density of a floc subjected to maximum mechanical dewatering pressures. These relationships describe the relative distribution of water and dry solids in aggregates, floc, and dewatered floc, respectively. The four parameters are defined below. Sample calculations may be found in Appendix B.

$$1. \quad \frac{\phi_a}{\phi_k} = \frac{\text{Undeformed aggregate volume}}{\text{Volume of dry solids in aggregate}}$$

This ratio was previously defined as the AVI. It provides a measure of the total aggregate water content.

$$2. \quad \frac{\phi_a}{\phi_f} = \frac{\text{Undeformed aggregate volume}}{\text{Undeformed floc volume}}$$

This parameter was first introduced by Michaels and Bolger (6) to quantify the volume of water present when comparing the floc structure and

aggregate structure.

$$3. \quad \frac{\phi_f}{\bar{\phi}_k} = \frac{\text{Undeformed floc volume}}{\text{Volume of dry solids in floc}}$$

This term is analagous to the AVI, but pertains only to the floc water content. Therefore,  $\phi_f/\bar{\phi}_k$  is defined as the floc volume index, (FVI).

$$4. \quad \frac{\phi_f}{\bar{\phi}_k} = \frac{\text{Dewatered (15 bar) floc volume}}{\text{Volume of dry solids in dewatered floc}}$$

This parameter provides a measure of the internal water remaining in a sludge after maximum mechanical dewatering.

Calculated values of these parameters are presented in Table 9. Values could not be calculated for the pure  $\text{CaCO}_3$  or glass bead suspensions since floc densities were not measured or reported by Javaheri (17). In research conducted by Vollrath-Vaughn (3), three of these parameters were calculated for similar sludge-types. The results were similar to the values calculated for Table 9, lending credibility to the experimental data gathered and to the reproducibility of the parameters.

TABLE 9

Calculated Values of Volume Fractions Applicable to  
Quantification of Sludge Water-Types

Sludge Type	$\frac{\phi_a}{\phi_k}$	$\frac{\phi_a}{\phi_f}$	$\frac{\phi_f}{\phi_k}$	$\frac{\phi_{f'}}{\phi_k}$
Ferric	1380	106	13	5.3
Unc Alum	164	16.4	10	5.6
Cond Alum	70	8.8	8	5.3
Lime	21	10.5	2	1.4

The data in Table 9 reveal that ferric aggregates contained much more water than either alum or lime aggregates. However, since the water content of the ferric hydroxide sludge was so high, only a small sample was collected on the filter paper after vacuum filtration. This extremely small sample may have misrepresented actual conditions, leading to the calculation of an uncharacteristically high AVI value.

An estimation of interfloc/intra-aggregate water is provided by the ratio of  $\phi_a/\phi_f$ . According to a previous study (3), this value is indicative of the water removed during mechanical dewatering. This research supports this statement, but adds that the relative amount of removal accomplished by mechanical dewatering methods is, to a certain degree, a function of the applied pressure differential.

The water most difficult to remove from dry sludge solids is represented by the last two columns in Table 9. The parameter  $\phi_f/\phi_k$  measures intrafloc water, removable only with high-pressure dewatering equipment. The ratio of  $\phi_f/\phi_k$  is indicative of internal water that remains after high-pressure dewatering. Comparison reveals that the three metal hydroxide sludges yielded similar values, all exceeding calculated values for lime. This fact provides insight into the nature of hydroxide versus non-hydroxide sludges. High internal

and chemically-bound water contents in hydroxide sludges are characteristic, largely due to the water of hydration associated with metal hydroxide precipitates. This chemical reaction tightly binds water to the dry sludge solids, creating a higher internal water content. However, lime sludge (essentially  $\text{CaCO}_3(\text{s})$ ) has a lower fraction of intrafloc and internal water, partly due to a decreased quantity of hydration water. This observation was also noted by Vollrath-Vaughn (3).

From these observations certain hypotheses concerning dewatering behavior in sludges were made:

1. Dewatering characteristics were a function of aggregate and floc densities. Lime sludge reached the highest solids concentration and floc volume content during dewatering. Its aggregate and floc densities measured higher than the other sludges. The relation between density and extent of dewatering was also seen in the alum and ferric sludges; the higher the aggregate and floc densities, the greater the extent of dewatering.

2. Dewatering characteristics were related to water-type. The conditioning of sludges is practiced to improve dewatering behavior. Evidence indicated that conditioning reduced the quantity of interfloc/intra-aggregate water, while increasing the extent of dewatering.

## V. CONCLUSION

The intent of this research was to study sludge dewatering behavior through the pursuit of three objectives. First, a technique was required to measure sludge floc density in the laboratory. This study attempted to improve existing laboratory methodology in order to include this important micro-property in sludge analyses. Assuming this technique did provide a credible floc density measurement, it was then possible to monitor and compare changes in fundamental sludge properties during dewatering. This information allowed the examination of existing water distribution models, resulting in the formulation of a separate model.

Based on the information collected during this research, the following conclusions were generated:

1. Sludge thickening rates are dependant upon a number of interrelated parameters. Specifically, settling velocities were shown to be influenced by aggregate volume fractions, sludge density, suspension porosity, and the total surface area occupied by sludge aggregates.

2. The extent of mechanical dewatering is impacted by similar parameters: namely, floc volume fractions, sludge density, cake porosity, and the total

surface area occupied by sludge floc.

3. From the formulated model of water distribution during the dewatering process, batch thickened solids could be composed of aggregates with a small amount of interaggregate water removed. Mechanical dewatering by centrifugation and vacuum filtration removes significant amounts of interfloc/intra-aggregate water, but may not disrupt the characteristic floc structure. Finally, high-pressure methods of mechanical dewatering remove certain amounts of intrafloc water, resulting in the possible deformation of floc structure and the production of a denser floc. The water remaining after maximum mechanical dewatering is composed to a significant degree of chemically bound, internal water.

A wealth of research is available to continue the study of micro-properties during dewatering. The suggested laboratory technique requires further refinement and definition. Further investigation of the interrelated parameters mentioned above is of importance in analyzing and improving gravity thickening and mechanical dewatering behavior in sludges. Also, a better understanding of the forces binding different water-types to dry sludge solids may lead to the improvement of dewatering techniques.



## VI. BIBLIOGRAPHY

1. Graf, W. H., "Hydraulics of Sediment Transport," McGraw-Hill, New York, (1971).
2. Pharmacia Fine Chemicals AB, "Percoll Methodology and Applications." Pharmacia Fine Chemicals AB, Box 175, S-751 04, Uppsala 1, Sweden.
3. Vollrath-Vaughn, Jean-Ann, "Metal Sludge Thickening Characteristics." M.S. Thesis. Virginia Polytechnic and State University, Blacksburg, VA (1984).
4. Mueller, J. A., K. G. Voelkel, and W. C. Boyle, "Nominal Diameter of Floc Related to Oxygen Transfer." Journal of the Sanitary Engineering Division, A. S. C. E., 92 (1966).
5. Lagvankar, Ashok L., and Robert S. Gemmell, "A Size-Density Relationship for Floccs." Journal of the American Water Works Association, 60, 1040 (1968).
6. Michaels, Alan S., and Justin C. Bolger, "Settling Rates and Settling Volumes of Flocculated Kaolin Suspensions." Industrial and Engineering Chemistry Fundamentals, 1, 24 (1962).
7. Javaheri, Ali R., and Richard I. Dick, "Aggregate Size Variations During Thickening of Activated Sludge." Journal Water Pollution Control Federation, 41, R197 (1969).
8. Richardson, J. F., and W. N. Zaki, "Sedimentation and Fluidization: Part I." Transactions Institution of Chemical Engineers, 32, 35 (1954).
9. Clark, John W., Warren Viessman, Jr., and Mark J. Hammer, Water Supply and Pollution Control, Third Edition. Harper & Row Publishers, Inc., New York, N. Y. (1977).
10. Knocke, William R. "Effects of Floc Volume Variations on Activated Sludge Thickening Characteristics." Submitted for Publication in Journal Water Pollution Control Federation, (1985).
11. Knocke, W. R., M. M. Ghosh, and J. T. Novak, "Vacuum Filtration of Metal Hydroxide Sludges." Journal of the Environmental Engineering Division, A. S. C. E., 106, 363 (1980).

12. Vesilind, P. A., Treatment and Disposal of Wastewater Sludges, Second Edition. Ann Arbor Science, Inc., Ann Arbor, Michigan (1979).
13. Gale, R. S., "Filtration Theory with Special Reference to Sewage Sludges." Water Pollution Control, 622 (1967).
14. Möller, U. K., "Water Binding." Sludge Characteristics and Behavior. J. B. Carberry, and A. J. Englands, Jr. (Eds.), NATO ASI Ser. E, No. 66, Martinus Nijhoff Publishers, The Hague, Netherlands (1983).
15. Environmental Protection Agency, "Dewatering Municipal Wastewater Sludges." Office of Research and Development, Municipal Environmental Research Laboratory, Cincinnati, Ohio (1982).
16. Wakeland, Douglas L., The Effect of Certain Sludge Floc Properties on the Dewatering Characteristics of Biological and Chemical Waste Sludges. M. S. Thesis. Virginia Polytechnic Institute and State University, Blacksburg, VA (1982).
17. Javaheri, Ali Rasool, Continuous Thickening of Non-Ideal Suspensions. Ph.D. Thesis. University of Illinois, Urbana-Champaign, Illinois (1971).

APPENDIX A

Data from gravity thickening tests: sludge concentrations and corresponding settling velocities.

(1.) Ferric sludge	%SS	$V_g$ , (cm/min)
	0.11	0.16
	0.09	0.67
	0.07	1.53
	0.06	1.81
	0.05	2.57
	0.04	2.97
(2.) Uncond. Alum	0.60	1.01
	0.45	1.59
	0.38	2.60
	0.30	2.89
	0.23	4.68
(3.) Cond Alum	1.05	1.24
	0.88	2.13
	0.70	2.40
	0.78	1.54
	0.61	3.06
(4.) Lime sludge	4.95	0.59
	4.54	0.61
	4.13	0.72
	3.63	0.94
	3.30	1.50

**The vita has been removed from  
the scanned document**